Nouveaux développements dans l'artérite à cellules géantes et la pseudopolyarthrite rhizomélique

Daniel Blockmans
Service de médecine interne, Hôpital universitaire Gasthuisberg
Louvain, Belgique

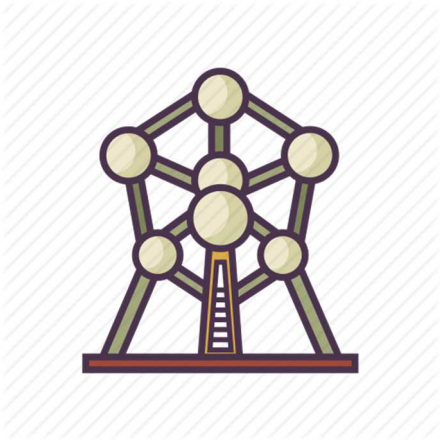

GFEV, Paris, 29 Mars 2018

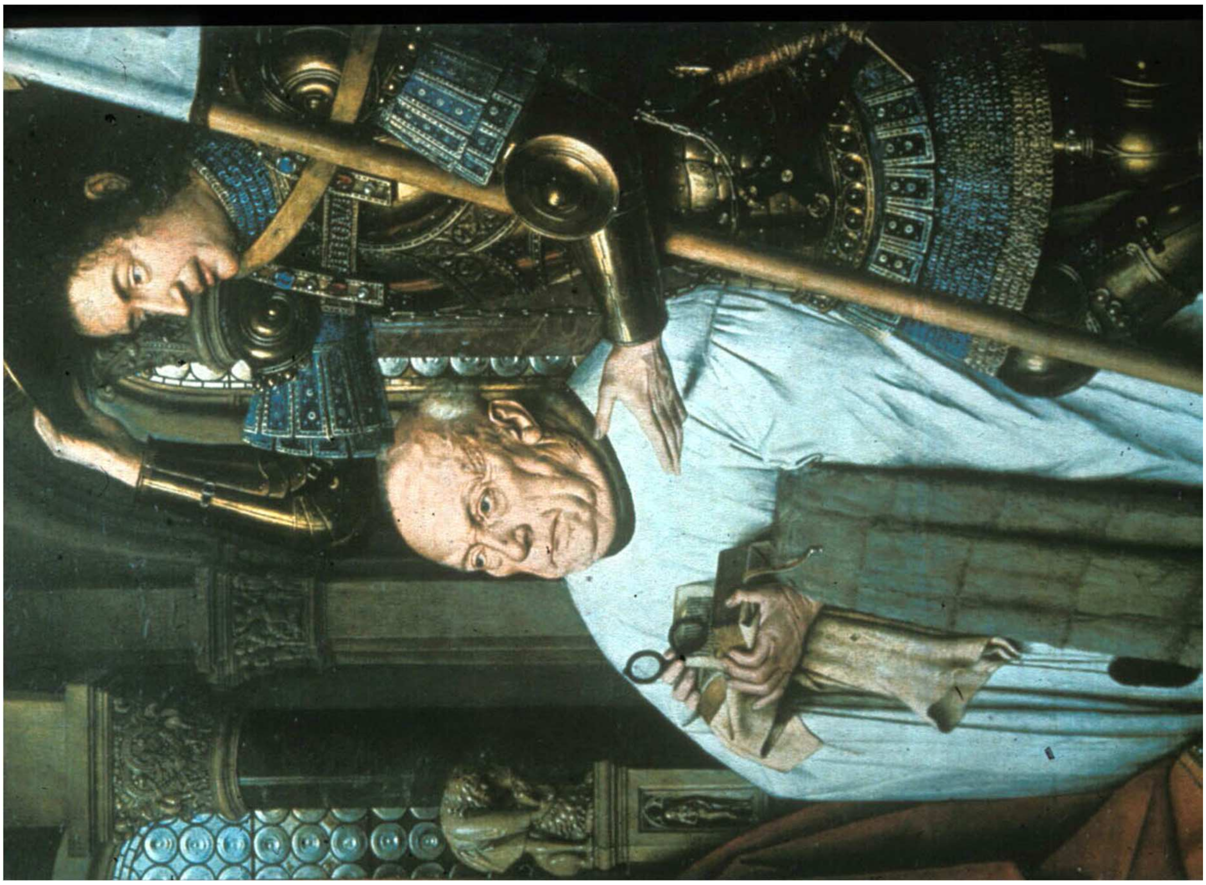

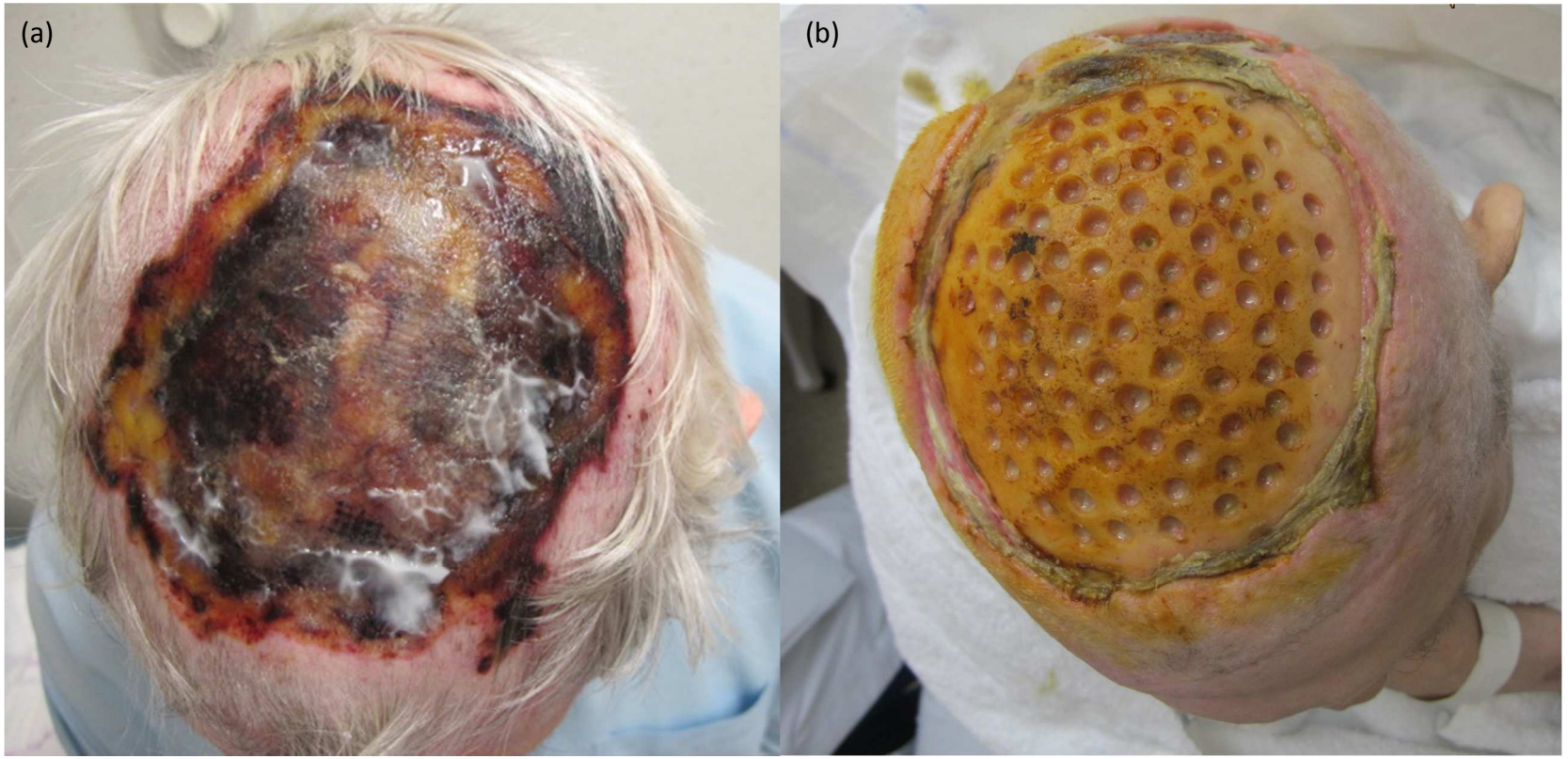

Fig.1 (a) massive necrosis of scalp tissue (b) after debridement with punctiform abrasion of the tabula externa

Mortality causes and trends associated with giant cell arteritis: analysis of the French national death certificate database (1980-2011).

Aouba A, Gonzalez Chiappe S, Eb M, Delmas C, de Boysson H, Bienvenu B, Rey G, Mahr A.

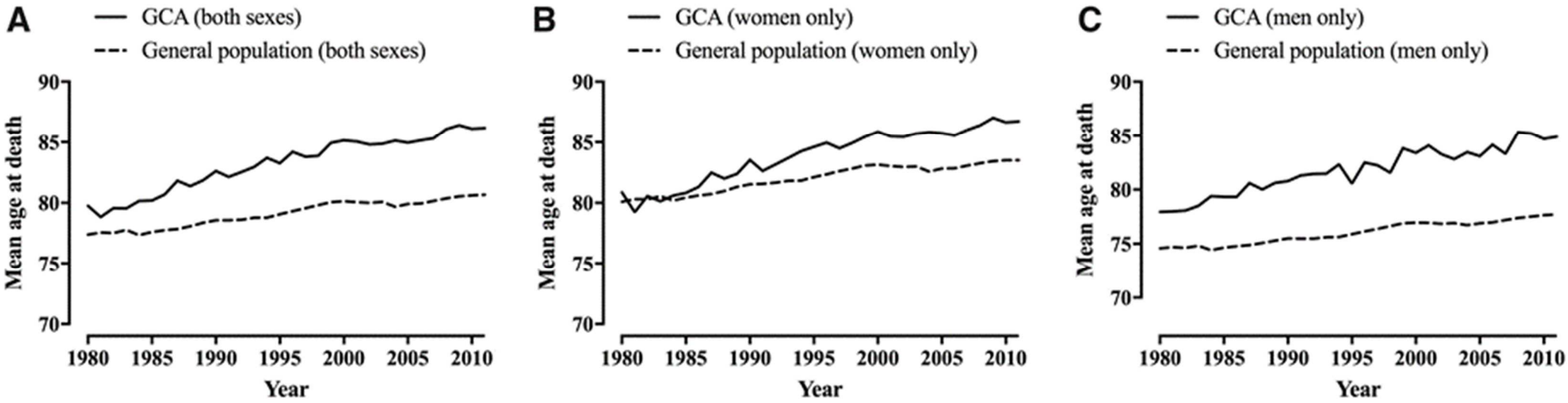

Rheumatology (Oxford). 2018 Mar 14

Mortality causes and trends associated with giant cell arteritis: analysis of the French national death certificate database (1980-2011).

Aouba A, Gonzalez Chiappe S, Eb M, Delmas C, de Boysson H, Bienvenu B, Rey G, Mahr A.

Underlying causes of death (ICD-10 codes)	Observed no of deaths (%)		SMOR
	GCA (*N* = 4427)	General population (*N* = 5 653 629)	(95% CI)
Certain infectious and parasitic diseases (A00–B99)	171 (3.86)	107 542 (1.90)	1.84 (1.51, 2.25)
Malignant neoplasms (C00–C80/C97)	373 (8.43)	1 429 175 (25.27)	0.47 (0.40, 0.56)
Malignant neoplasms, stated or presumed to be primary, of lymphoid, haematopoietic and related tissue (C81–C96)	84 (1.90)	137 432 (2.43)	0.85 (0.65, 1.09)
Diabetes mellitus (E10–E14)	177 (4.00)	127 132 (2.25)	1.65 (1.35, 2.00)
Organic, including symptomatic, mental disorders (F00–F09)	162 (3.66)	141 650 (2.51)	1.02 (0.83, 1.26)
Other degenerative diseases of the nervous system (G30–G32)	175 (3.95)	181 255 (3.21)	0.89 (0.73, 1.09)
Hypertensive diseases (I10–I15)	196 (4.43)	97 609 (1.73)	2.02 (1.67, 2.45)
Ischaemic heart diseases (I20–I25)	473 (10.68)	450 162 (7.96)	1.26 (1.08, 1.48)
Pulmonary heart disease and diseases of pulmonary circulation (I26–I28)	66 (1.49)	60 231 (1.07)	1.18 (0.89, 1.55)
Other forms of heart disease (I30–I34/I36–I45/I47–I52)	422 (9.53)	477 658 (8.45)	0.91 (0.77, 1.07)
Non-rheumatic aortic valve disorders (I35)	67 (1.51)	41 138 (0.73)	1.68 (1.27, 2.19)
Cerebrovascular diseases (I60–I69)	482 (10.89)	392 687 (6.95)	1.30 (1.11, 1.53)
Aortic aneurysm and dissection (I71)	58 (1.31)	32 102 (0.57)	2.72 (2.01, 3.62)
Influenza and pneumonia-other acute lower respiratory infections (J10–J22)	150 (3.39)	164 492 (2.91)	0.91 (0.74, 1.12)
Chronic lower respiratory diseases (J40–J47)	114 (2.58)	104 688 (1.85)	1.40 (1.11, 1.75)
Vascular disorders of intestine (K55)	41 (0.93)	27 252 (0.48)	1.64 (1.16, 2.26)
Paralytic ileus and intestinal obstruction without hernia (K56)	42 (0.95)	32 720 (0.58)	1.29 (0.92, 1.78)
External causes of morbidity and mortality (V01–Y98)	232 (5.24)	291 564 (5.16)	Control

SMOR calculations used the general population ⩾ 55 years old as the non-exposed group and deaths related to 'external causes of morbidity and mortality' as the control group. ICD-10: International Classification of Diseases, 10th revision; SMOR: standardized mortality odds ratios.

Rheumatology (Oxford) 2018 Mar 14

New developments in GCA and PMR

- Gold standard for diagnosis ??
- Pathogenesis
- Positron emission tomography as diagnostic tool
- New treatments

The Role of Ultrasound Compared to Biopsy of Temporal Arteries in the Diagnosis and Treatment of Giant Cell Arteritis (TABUL): a diagnostic accuracy and cost-effectiveness study

Luqmani R, Lee E, Singh S, Gillett M, Schmidt W A, Bradburn M, Dasgupta B, Diamantopoulos A P, Forrester-Barker W, Hamilton W, Masters S, McDonald B, McNally E, Pease C, Piper J, Salmon J, Wailoo A, Wolfe K & Hutchings A.

Results

We developed and implemented an ultrasound training programme for diagnosing suspected GCA. We recruited 430 patients with suspected GCA. We analysed 381 patients who underwent both ultrasound and biopsy within 10 days of starting treatment for suspected GCA and who attended a follow-up assessment (median age 71.1 years; 72% female). The sensitivity of biopsy was 39% [95% confidence interval (CI) 33% to 46%], which was significantly lower than previously reported and inferior to ultrasound (54%, 95% CI 48% to 60%); the specificity of biopsy (100%, 95% CI 97% to 100%) was superior to ultrasound (81%, 95% CI 73% to 88%). If we scanned all suspected patients and performed biopsies only on negative cases, sensitivity increased to 65% and specificity was maintained at 81%, reducing the need for biopsies by 43%. Strategies combining clinical judgement (clinician's assessment at 2 weeks) with the tests showed sensitivity and specificity of 91% and 81%, respectively, for biopsy and 93% and 77%, respectively, for ultrasound; cost-effectiveness (incremental net monetary benefit) was £485 per patient in favour of ultrasound with both cost savings and a small health gain. Inter-rater analysis revealed moderate agreement among sonographers (intraclass correlation coefficient 0.61, 95% CI 0.48 to 0.75), similar to pathologists (0.62, 95% CI 0.49 to 0.76).

Health Technol Assess 2016; 20: 1-238

Poor Predictive Value of Isolated Adventitial and Periadventitial Infiltrates in Temporal Artery Biopsies for Diagnosis of Giant Cell Arteritis

Le Pendu C
Meignin V
Gonzalez-Chiappe S
Hij A
Galateau-sallé F
Mahr A

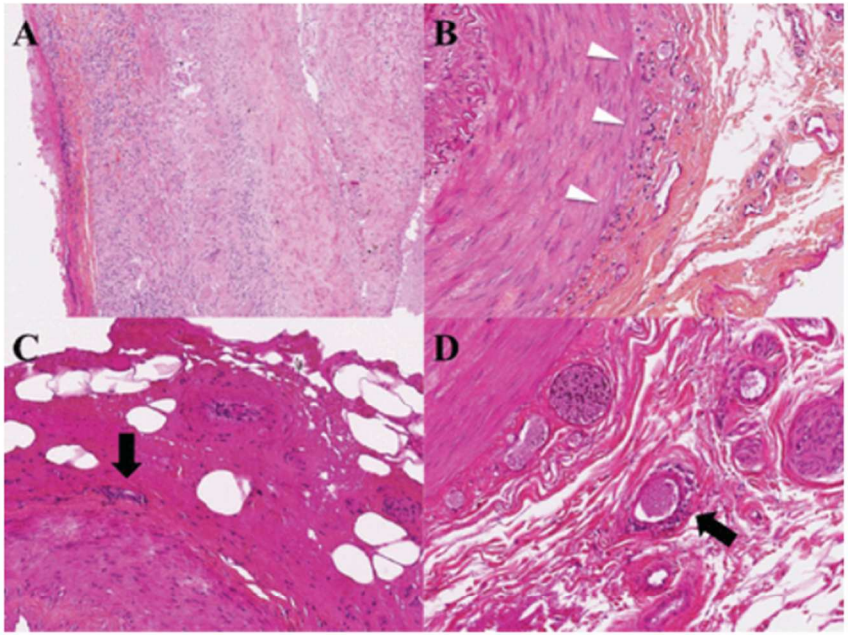

Figure 1. Download figure | Open in new tab | Download powerpoint

Examples of histopathological features found in the analyzed temporal artery biopsies. (A) Classic giant cell arteritis with prominent mononuclear cell infiltrate of the media, giant cells, and fibrosis. (B) Inflammation limited to adventitia with scattered mononuclear infiltrate (arrowheads) in a 69-year-old man with no acute illness diagnosed and spontaneous recovery. (C) Vasa vasorum vasculitis with mononuclear perivasculitis of an intraadventitial vessel (arrow) in an 84-year-old man diagnosed with rectal adenocarcinoma. (D) Small-vessel vasculitis with perivascular mononuclear infiltrate of a periadventitial vessel (arrow) in a 77-year-old man with no acute illness diagnosed and spontaneous recovery. H&E staining × 100 (A) and × 250 (B–D) .

J Rheumatol 2017; 44: 1039-44

GCA : pathogenesis

Pathophysiology of GCA

Normal Artery

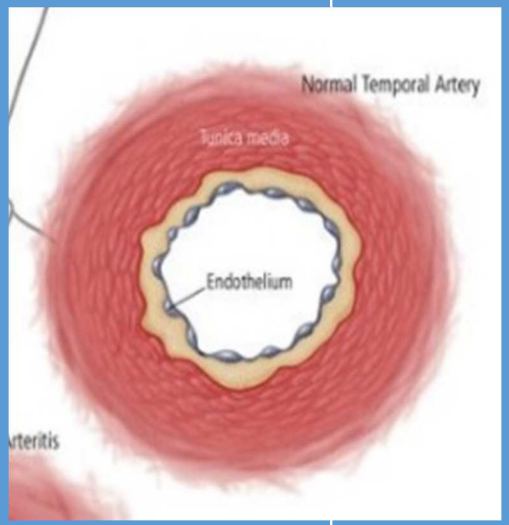

Giant cell arteritis

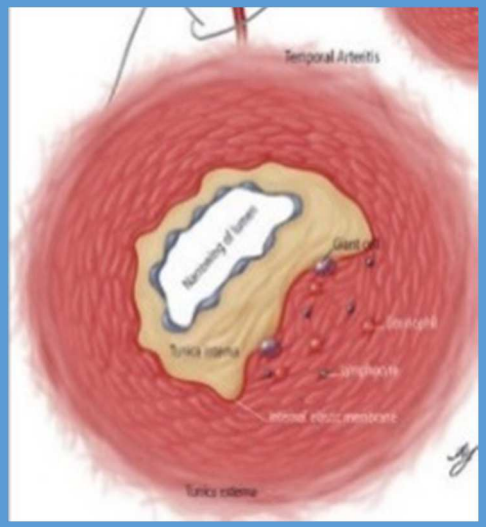

In GCA the temporal arteries become inflamed leading to swelling of the blood vessel wall and narrowing of the blood vessel lumen, decreasing blood supply. The cause of GCA is unknown, although the immune system attacks the arteries. A number of cells contribute to this inflammation including dendritic cells, T cells, and macrophages. In the normal artery, vascular dendritic cells are immature. In GCA, the dendritic cells are activated leading to a recruitment of macrophages and CD4+ T cells. CD4 + T cells differentiate into Th17 cells or Th1 cells. Th17 cells are responsible for systemic manifestation of the disease and Th1 cells (along with IFN-g) activate macrophages and are involved in destroying the structural integrity of the vessel wall. Dysregulated vascular smooth muscle cells migrate toward the lumen forming intimal hyperplasia

GCA : pathogenesis

- Inflammation starts at the junction between the media layer and the adventitia, where activated dendritic cells recruit CD4+ lymphocytes from the vasa vasorum and stimulate them
- These T-cells, enriched in type 1 and type 17 T-helper cells, release IL12, IL17 and interferon-gamma, which activates macrophages which are also attracted from the vasa vasorum and invade the media layer
- These macrophages synthesize PDGF, leading to intimal hyperplasia, and matrix metalloproteinases and free oxygen radicals which cause vessel wall damage

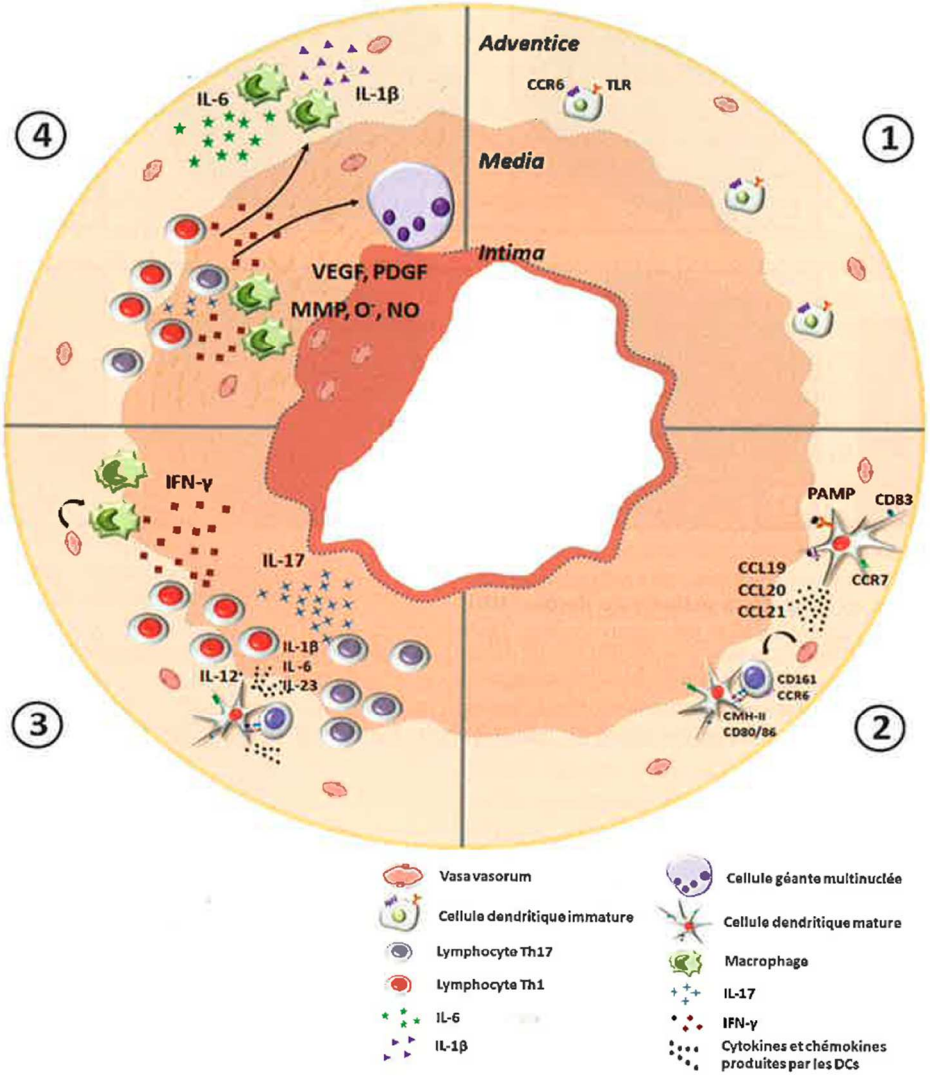

Samson and Bonnotte. Presse Med 2012; 41: 937-947.

PMR and GCA : pathogenesis

- Macrophages in the arterial wall and the synovium produce the proinflammatory cytokines TNF, IL1 and IL6, which produce the constitutional symptoms of GCA and PMR
- Increased plasma levels of IL6, IL2, IL1beta, VEGF, PDGF and monocyte chemoattractant protein 1

Immune mechanisms in medium and large-vessel vasculitis

Weyand CM, Goronzy JJ

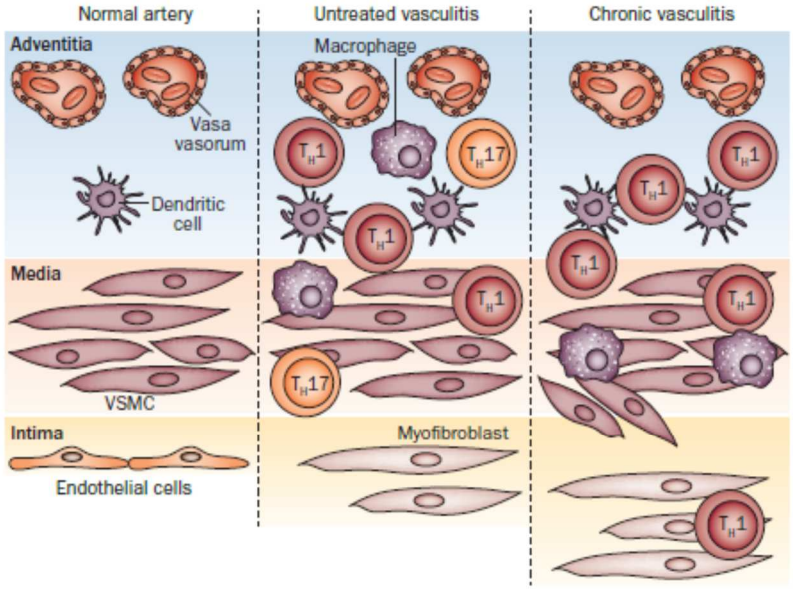

Figure 1 | T_H1-cell-mediated and T_H17-cell-mediated immunity in giant cell arteritis. The walls of human arteries are multilayered, with an endothelial barrier in the intima, sheets of VSMCs in the media and the vasa vasorum network in the adventitia. Endogenous vascular dendritic cells populate the adventitia (left) and are responsible for the recruitment of T cells and macrophages into the tissue niche. In early and untreated vasculitis, IFN-γ–producing T_H1 cells and IL-17-secreting T_H17 cells are abundant, surrounded by macrophages (middle). Corticosteroid therapy diminishes T_H17 cells, but cannot clear T_H1 cells from the vascular lesions (right). Dysregulated VSMCs migrate towards the lumen and lay down to form lumen-stenosing intimal hyperplasia. Abbreviations: T_H1 (cell), type 1 helper T (cell); T_H17 (cell), type 17 helper T (cell); VSMC, vascular smooth muscle cell.

Nature Reviews Rheumatology, 2013 Dec, Vol.9(12), pp.731-740

GCA : pathogenesis : what is the antigen ?

- Many viruses have been suspected (varicella-zoster virus, Epstein-Barr virus, cytomegalovirus, HHV-6, parvovirus B19,…) but none confirmed
- Chlamydia pneumoniae : idem
- Probably an auto-antigen, eg heat shock proteins (HSP) from anti-endothelial cell antibodies (AECAs)

Immunoinhibitory checkpoint deficiency in medium and large vessel vasculitis.

Zhang H, Watanabe R, Berry GJ, Vaglio A, Liao YJ, Warrington KJ, Goronzy JJ, Weyand CM.

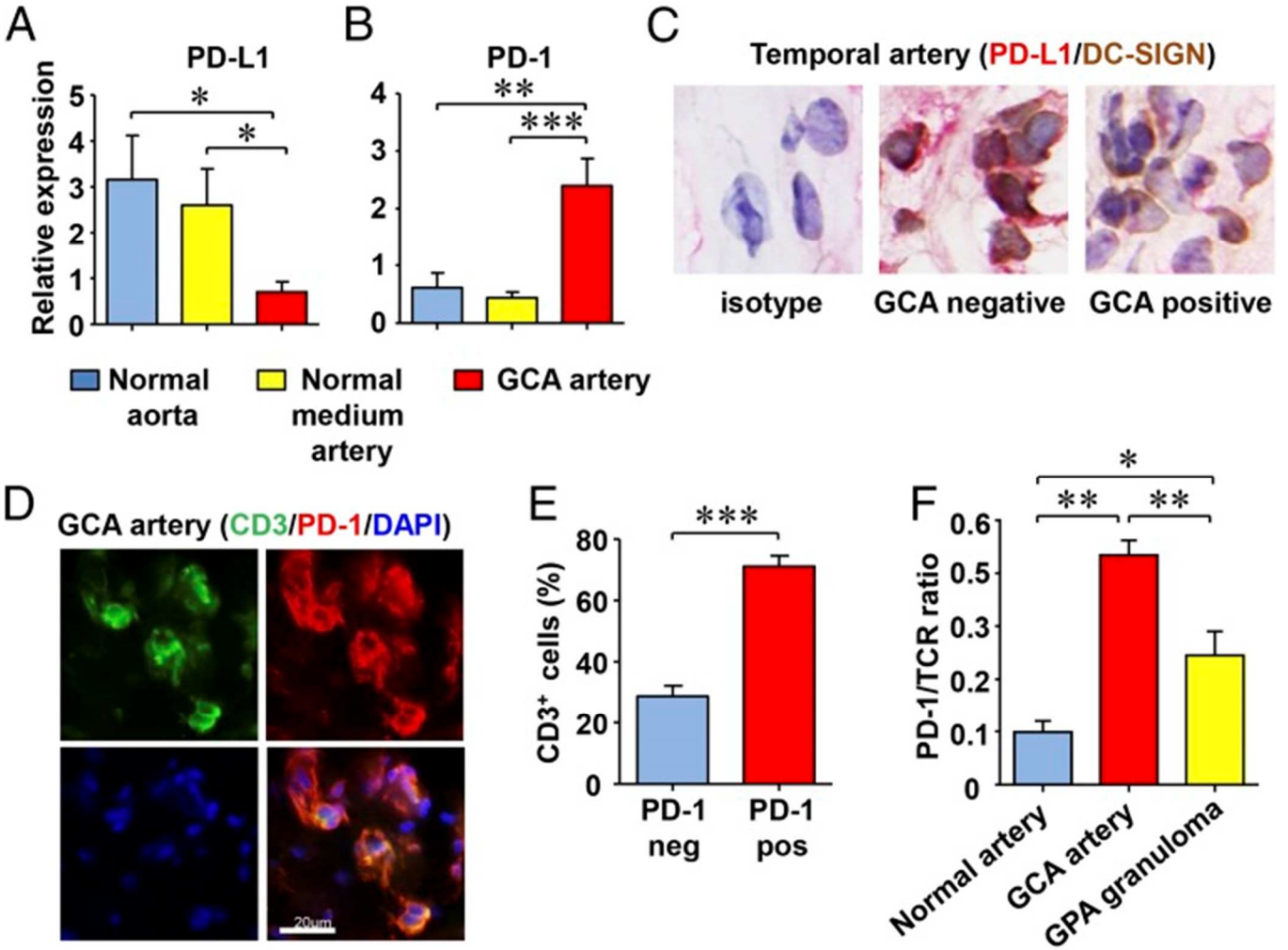

PD-L1lo DC and PD-1+ T cells in GCA. RNA was extracted from normal aortic wall, noninflamed medium-sized arteries, and from GCA-affected arteries (n = 10 each). In patients with GPA, granulomatous lesions in the lung and in the skin were examined (n = 10). (A) Expression of PD-L1 transcripts and (B) PD-1 transcripts was quantified by RT-PCR. (C) Tissue sections from temporal arteries were stained with anti–PD-L1 (red) and anti–DC-SIGN (brown) antibodies. (D) Tissue sections from GCA affected temporal arteries were stained with anti–PD-1 (red) and anti-CD3 (green) antibodies. Alexa Fluor 488 anti-rabbit (1:100) and Alexa Fluor 546 anti-mouse (1:100) secondary antibodies were used to visualize primary antibody binding. Representative images are shown. (E) Frequencies of CD3+PD-1+ T cells were quantified in vascular wall cross-sections. (F) Tissue expression of TCR and PD-1 was assessed in nonvasculitic and vasculitis-affected tissues (GCA or GPA). Ratios of PD-1/TCR are presented. Data are mean ± SEM from 10 different patient samples. *P < 0.05, **P < 0.01, ***P < 0.001. (Original magnification: 600×.)

Proc Natl Acad Sci U S A. 2017 Feb 7;114:E970-E979.

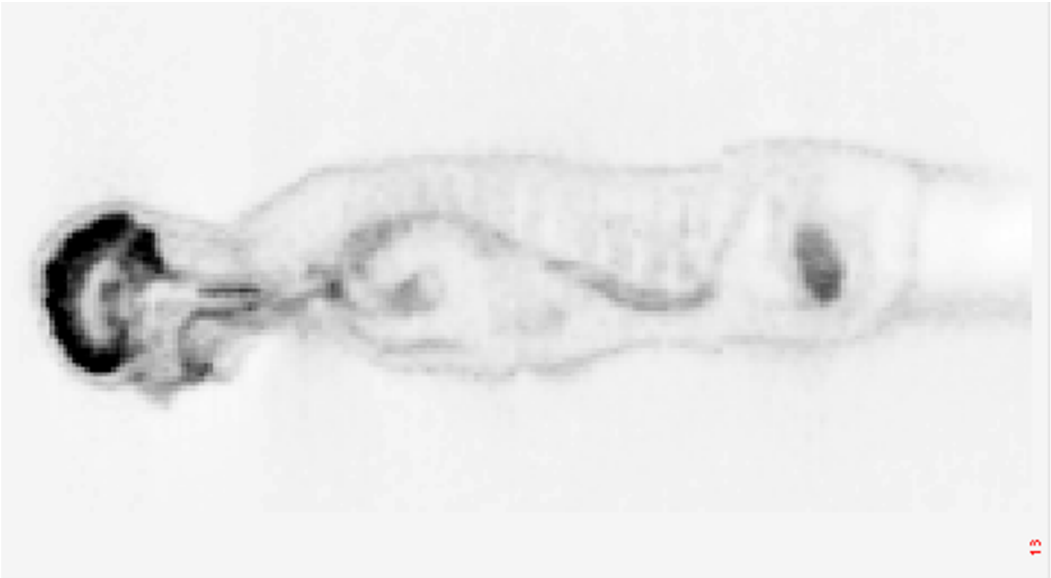

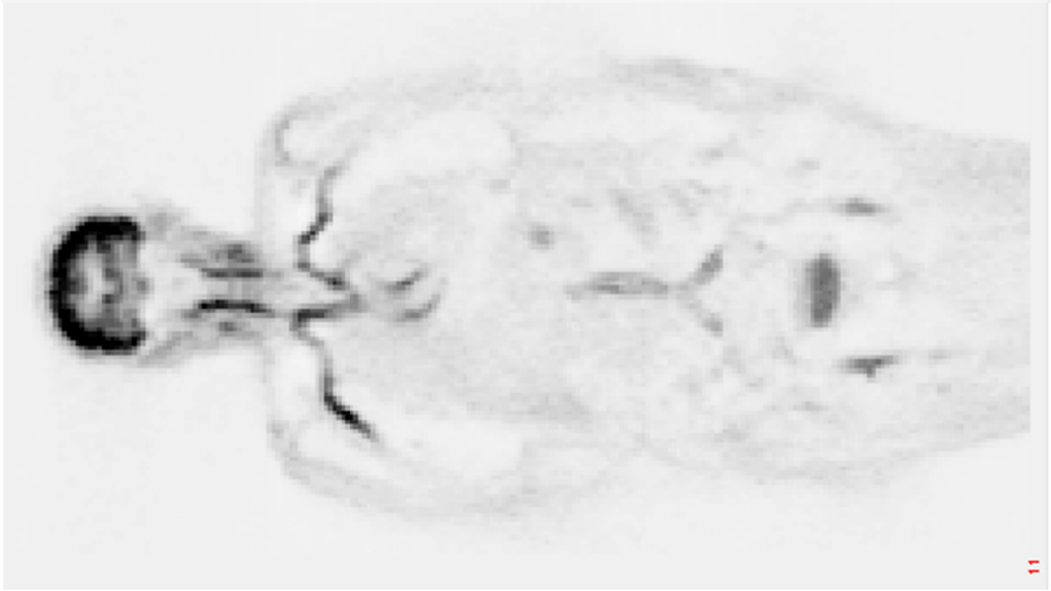

Relationship between fluorodeoxyglucose uptake in the large vessels and late aortic diameter in giant cell arteritis

D. Blockmans[1], W. Coudyzer[2], S. Vanderschueren[1], S. Stroobants[3], D. Loeckx[4], S. Heye[2], L. De Ceuninck[3], G. Marchal[2] and H. Bobbaers[1]

Objective. GCA carries an increased risk of developing thoracic aortic aneurysms. Previous work with fluorodeoxyglucose (FDG)-PET has shown that the aorta is frequently involved in this type of vasculitis. We wanted to investigate whether there is a correlation between the extent of vascular FDG uptake during the acute phase of GCA and the aortic diameter at late follow-up.

Methods. All patients with biopsy-proven GCA who ever underwent an FDG-PET scan in our centre were asked to undergo a CT scan of the aorta. The diameter of the aorta was measured at six different levels (ascending aorta, aortic arch, descending aorta, abdominal suprarenal, juxtarenal and infrarenal aorta) and the volumes of the thoracic and of the abdominal aorta were calculated.

Results. Forty-six patients agreed to participate (32 females, 14 males). A mean of 46.7 ± 29.9 months elapsed between diagnosis and CT scan. All aortic dimensions were significantly smaller in women than in men, except for the diameter of the ascending aorta. Patients who had an increased FDG uptake in the aorta at diagnosis of GCA, had a significantly larger diameter of the ascending aorta ($P = 0.025$) and descending aorta ($P = 0.044$) and a significantly larger volume of the thoracic aorta ($P = 0.029$). In multivariate analysis, FDG uptake at the thoracic aorta was associated with late volume of the thoracic aorta ($P = 0.039$).

Conclusion. GCA-patients with increased FDG uptake in the aorta may be more prone to develop thoracic aortic dilatation than GCA patients without this sign of aortic involvement.

KEY WORDS: Giant cell arteritis, Temporal arteritis, Vasculitis, Large-vessel vasculitis, Aorta, Positron Emission tomography, Fluorodeoxyglucose, Aortic dilatation, Vascular inflammation, Aortic aneurysm.

Rheumatology 2008;47:1179–1184

Methods

- All patients with biopsy-proven GCA who ever (1996-2006) underwent a FDG-PET scan in our centre were asked to return and undergo a CT-scan of the aorta in the period January-July 2006
- Original FDG-PET scintigraphies were reread by two independent nuclear medicine specialists, who were unaware of CT-findings. Aortic FDG-uptake was reported as negative (score 0 or 1) or positive (score 2 or 3).
- The diameter of the aorta was measured at six different levels (ascending aorta, aortic arch, descending thoracic aorta, abdominal suprarenal, juxtarenal and infrarenal aorta) and the volume of the thoracic aorta and of the abdominal aorta were calculated

Blockmans et al, Rheumatology 2008

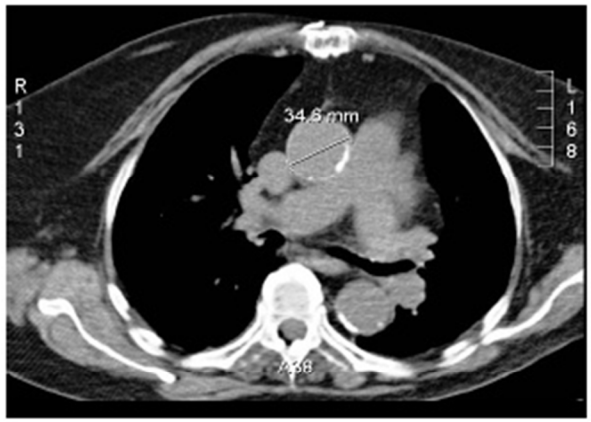

ascending aorta

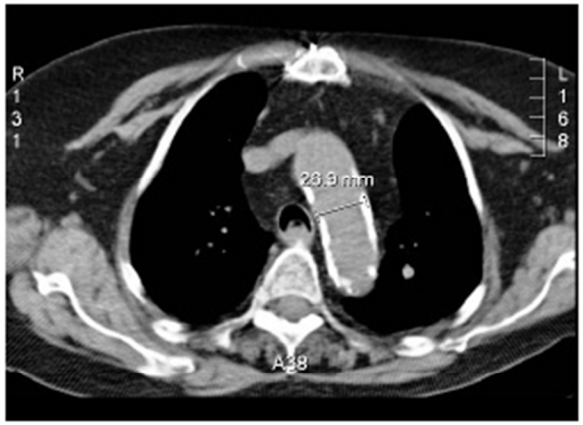

aortic arch

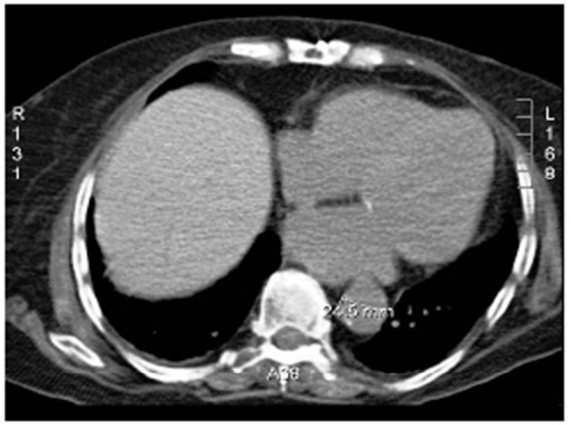

descending aorta

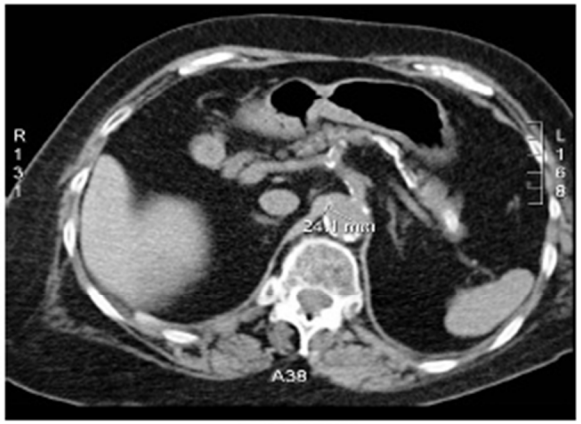

suprarenal

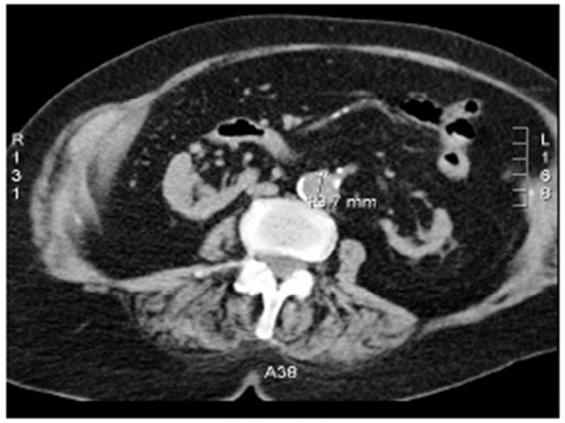

juxtarenal

abdominal aorta

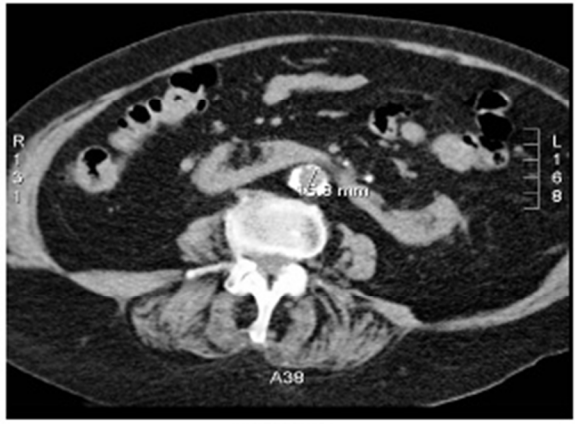

infrarenal

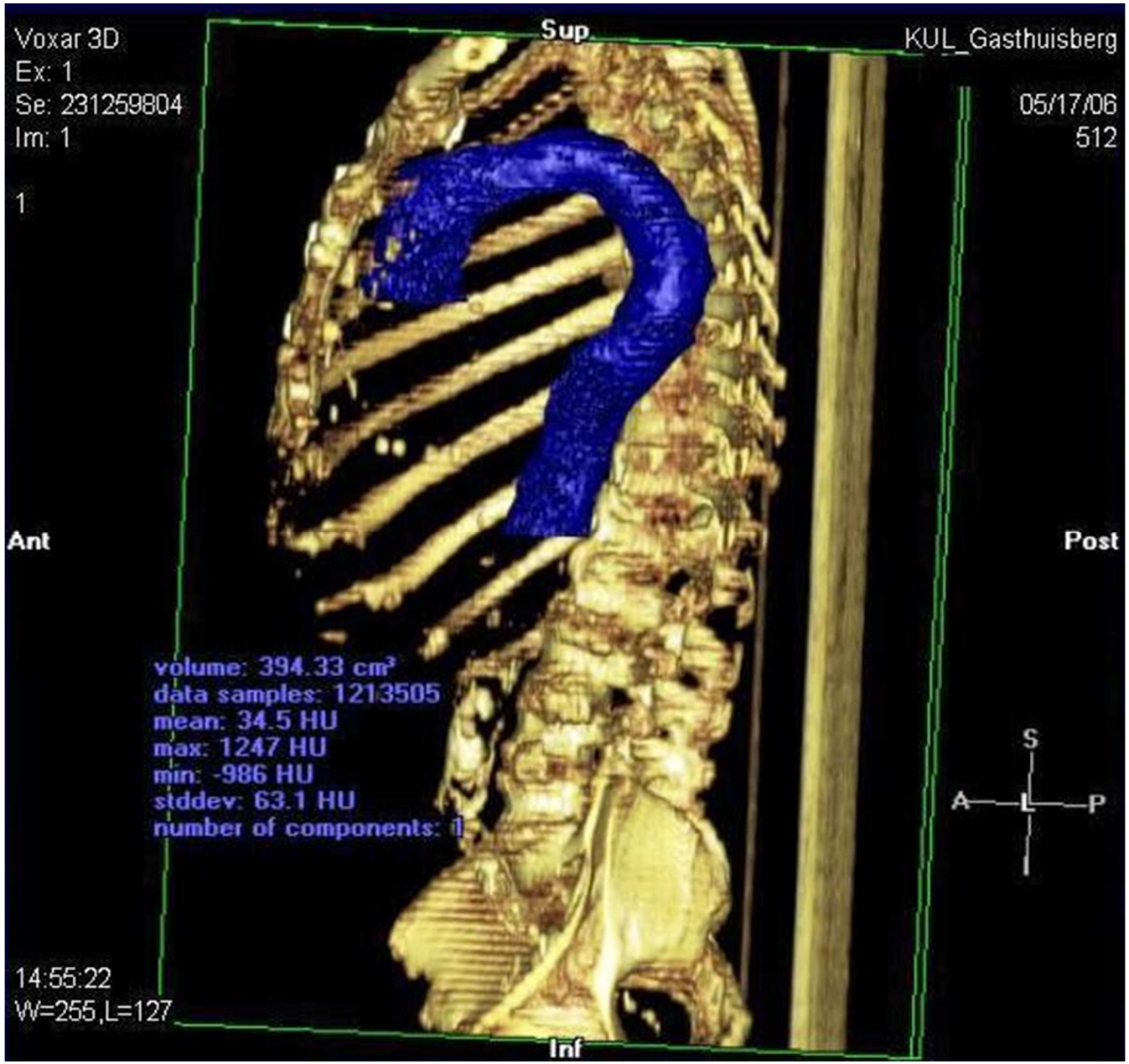
Voxar 3D
Ex: 1
Se: 231259804
Im: 1
1
Sup
KUL_Gasthuisberg
05/17/06
512
Ant
Post
volume: 394.33 cm³
data samples: 1213505
mean: 34.5 HU
max: 1247 HU
min: -986 HU
stddev: 63.1 HU
number of components: 1
S
A
L
P
14:55:22
W=255,L=127
Inf

Results : effect of initial FDG-uptake at the thoracic aorta on aortic dimensions

Aortic dimensions (mean ± SD)	FDG-uptake negative (n = 24)	FDG-uptake positive (n = 22)	p-value
Diameter ascending aorta (mm)	37.0 ± 2.8	40.4 ± 6.9	0.025
Diameter aortic arch (mm)	30.1 ± 3.6	31.2 ± 3.6	0.281
Diameter descending aorta (mm)	30.6 ± 4.0	33.5 ± 5.3	0.044
Volume thoracic aorta (cm^3)	253 ± 51	301 ± 81	0.029

Results : multivariate analysis

Dependent variable : volume thoracic aorta

- Gender : p = 0.252
- Age at CT-scan : p = 0.569
- Body length : p = 0.470
- Months elapsed since diagnosis : p = 0.572
- FDG-uptake at thoracic aorta : p = **0.039**

Observational Study

Medicine®

OPEN

^{18}F-fluorodeoxyglucose positron emission tomography and the risk of subsequent aortic complications in giant-cell arteritis

A multicenter cohort of 130 patients

Hubert de Boysson (MD, MSc)[a,*], Eric Liozon (MD)[b], Marc Lambert (MD, PhD)[c], Jean-Jacques Parienti (MD, PhD)[d], Nicolas Artigues (MD)[e], Loïk Geffray (MD)[f], Jonathan Boutemy (MD)[a], Yann Ollivier (MD)[a], Gwénola Maigné (MD)[a], Kim Ly (MD)[b], Damien Huglo (MD, PhD)[g], Eric Hachulla (MD, PhD)[c], Pierre-Yves Hatron (MD, PhD)[c], Achille Aouba (MD, PhD)[a], Alain Manrique (MD, PhD)[h], Boris Bienvenu (MD, PhD)[a]

Patient characteristics according to the presence or absence of aortic complications.

Characteristic	Total (n=130)	Aortic complications (n=9)	No aortic complication (n=121)	*P*
Demographic characteristics				
Women	85 (65)	5 (56)	80 (66)	0.72
Age	70 [53–86]	66 [56–76]	71 [50–86]	0.19
Cardiovascular risk factors				
Hypertension	60 (46)	2 (22)	58 (48)	0.18
Dyslipidemia	34 (26)	2 (22)	32 (26)	0.99
Diabetes mellitus	17 (13)	1 (11)	16 (13)	0.99
Smoking	26 (20)	3 (33)	23 (19)	0.38
Clinical manifestations				
Fever	45 (35)	3 (33)	42 (35)	0.99
Cephalic manifestations	108 (83)	7 (78)	101 (83)	0.65
Headaches	100 (77)	7 (78)	93 (77)	0.99
Ophthalmologic signs	29 (22)	1 (11)	28 (23)	0.68
Extracephalic manifestations	64 (49)	5 (56)	59 (49)	0.74
Polymyalgia rheumatica	49 (38)	5 (56)	44 (36)	0.99
Vascular bruits	15 (11)	1 (11)	14 (12)	
Limb claudication	5 (3)	—	5 (4)	—
Laboratory tests				
Erythrocyte sedimentation rate, mm	79 [14–135]	56 [33–75]	80 [14–135]	0.16
C-reactive protein, mg/L	116 [3–400]	80 [30–390]	119 [3–400]	0.25
Histological results				
Positive TAB	75/128 (59)	6 (67)	69 (57)	0.73
Other positive vascular histology	2/2 (100)	2 (22)	—	—
Positive PET	69 (53)	9 (100)	60 (50)	0.003
Dose of corticosteroids at diagnosis	50 [20–110]	60 [30–70]	50 [20–110]	0.26

PET = positron emission tomography, TAB = temporal artery biopsy.
All results are numbers (percentage) or medians [range].

De Boysson H, et al. Medicine 2016; 95: 26

Attenuation of Fluorine-18-Fluorodeoxyglucose Uptake in Large Vessel Giant Cell Arteritis after Short-Term High-Dose Steroid Treatment – a Diagnostic Window of Opportunity

Berit Dalsgaard Nielsen, Ib Tønder Hansen, Kresten Krarup Keller, Philip Therkildsen, et al.

Post-therapeutic LV-GCA diagnosis by 18F-FDG PET/CT

	PET3	PET10
PET positive	10/10	5/10

Median vascular composite score

	PET0	PET3	PET0	PET10
Aorta€	9 (9-9)	9 (6-9)	9 (9-9)	5 (3-6)*
Aortic branches#	6 (5-8)	4.5 (3-7)*	6.5 (6-8)	4 (3-5)*

PET positive was defined as vascular 18F-FDG uptake≥3. A vascular composite score in two different vascular domains was calculated by summarizing the grades for selected regions. Medians (interquartile range) in the two groups (PET3 or PET10, n=10 respectively) are presented. *Indicates that post-therapeutic vascular score was significantly different from pre-therapeutic score. €*Aortic: Aorta ascendens, aorta descendens and aortic arch.* #*Aortic branches: Vertebral, carotic and subclavian/axillary artery.*

Arthritis Rheumatol. 2016; 68 (suppl 10).

Repetitive 18F-FDG-PET/CT in patients with large-vessel giant-cell arteritis and controlled disease.

de Boysson H, Aide N, Liozon E, Lambert M, Parienti JJ, Monteil J, Huglo D, Bienvenu B, Manrique A, Aouba A.

OBJECTIVE:
18F-FDG PET/CT can detect large-vessel involvement in giant-cell arteritis (GCA) with a good sensitivity. In patients with clinically and biologically controlled disease, we aimed to assess how vascular uptakes evolve on repetitive FDG-PET/CT.

PATIENTS AND METHODS:
All included patients had to satisfy the 4 following criteria: 1) diagnosis of GCA was retained according to the criteria of the American College of Rheumatology or based on the satisfaction of 2 criteria associated with the demonstration of large-vessel involvement on FDG-PET/CT; 2) all patients had a positive PET/CT that was performed at diagnosis before treatment or within the first 10days of treatment; 3) another FDG-PET/CT was performed after at least 3months of controlled disease without any relapse; 4) patients were followed-up at least for 12months.

RESULTS:
Twenty-five patients (17 [68%] women, median age: 69 [65-78]) with large-vessel inflammation on a baseline FDG-PET/CT and with repetitive imaging during the period with controlled disease were included and followed-up for 62 [25-95] months. Four repeated procedures revealed total extinction of vascular uptakes at 11.5 [8-12] months after the first FDG-PET/CT. Eight PET/CT revealed decreased numbers of vascular uptakes, and 10 procedures revealed no changes. The 3 remaining procedures indicated worsening of the numbers of vascular uptakes in the absence of relapse.

CONCLUSIONS:
Our study revealed long-term persistent vascular uptake on repeated FDG-PET/CT in >80% of our GCA patients with large-vessel inflammation and clinical-biological controlled disease. Prospective studies are required to confirm these findings.

Eur J Intern Med. 2017; 46: 66-70.

^{18}F-Fluorodeoxyglucose–Positron Emission Tomography As an Imaging Biomarker in a Prospective, Longitudinal Cohort of Patients With Large Vessel Vasculitis

Peter C. Grayson,[1] Sara Alehashemi,[1] Armin A. Bagheri,[1] Ali Cahid Civelek,[2] Thomas R. Cupps,[3] Mariana J. Kaplan,[1] Ashkan A. Malayeri,[2] Peter A. Merkel,[4] Elaine Novakovich,[1] David A. Bluemke,[2] and Mark A. Ahlman[2]

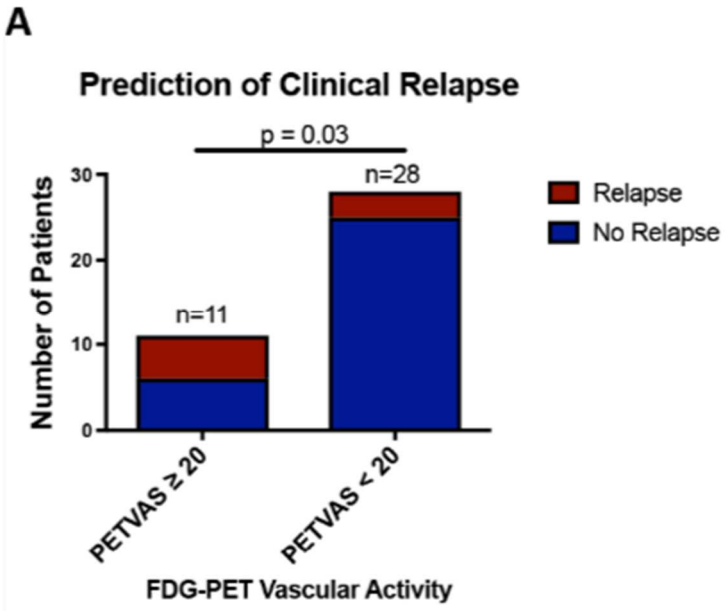

ARTHRITIS & RHEUMATOLOGY
Vol. 70, No. 3, March 2018, pp 439–449

Use of 18F-fluorodeoxyglucose positron emission tomography in the diagnosis of polymyalgia rheumatica-A prospective study of 99 patients.

Henckaerts L, Gheysens O, Vanderschueren S, Goffin K, Blockmans D.

METHODS

• We prospectively included 99 consecutive consenting patients with a possible diagnosis of PMR,

• Clinical probability was scored by the treating physician on a scale from 1 to 5, based on clinical symptoms and laboratory values .

• 18F-FDG-PET scanning was done before treatment with glucocorticoids; FDG-uptake was scored visually in 12 articular regions (score 0-2 per region): cervical and lumbar spinous processes, sternoclavicular joints, ischial tuberosities, greater trochanters, hips and shoulders (figure 1).

• A total skeletal score was calculated for every patient, by summing up the individual scores at the 12 different skeletal sites (total 0 to 24).

• The golden standard for a diagnosis of PMR was the judgment of an experienced clinician after at least six months of follow-up.

Rheumatology (Oxford). 2017 Oct 7. doi: 10.1093/rheumatology/kex376. [Epub ahead of print]

Use of 18F-fluorodeoxyglucose positron emission tomography in the diagnosis of polymyalgia rheumatica-A prospective study of 99 patients.

Henckaerts L, Gheysens O, Vanderschueren S, Goffin K, Blockmans D.

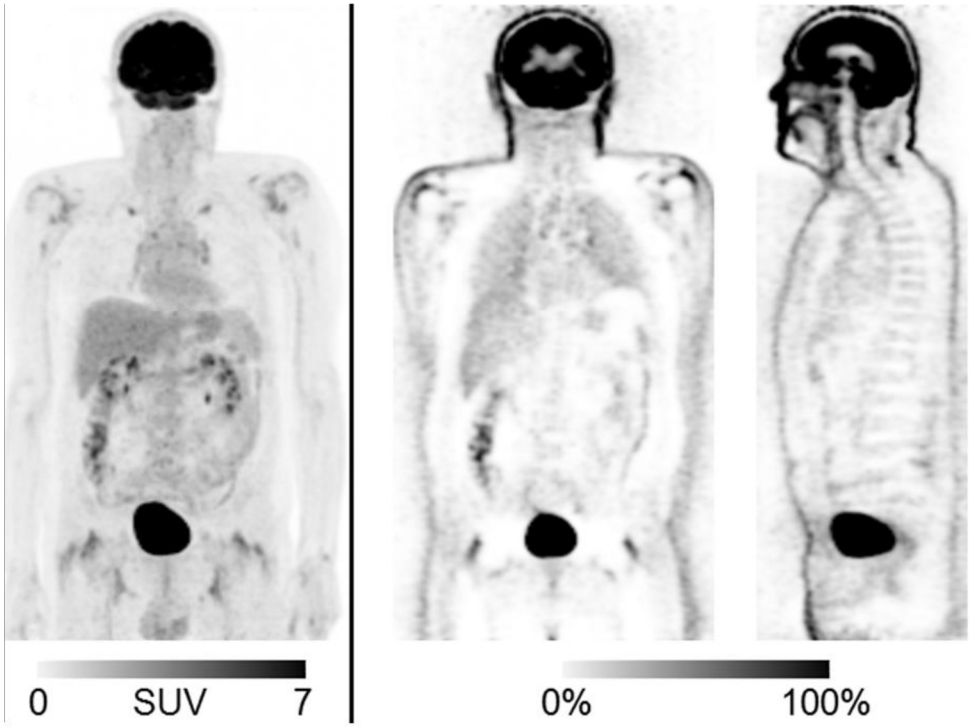

Figure 1: Example of a PET image in a PMR patient with a total skeletal score of 24 (maximal score).

Rheumatology (Oxford). 2017 Oct 7. doi: 10.1093/rheumatology/kex376. [Epub ahead of print]

Use of 18F-fluorodeoxyglucose positron emission tomography in the diagnosis of polymyalgia rheumatica-A prospective study of 99 patients.

Henckaerts L, Gheysens O, Vanderschueren S, Goffin K, Blockmans D.

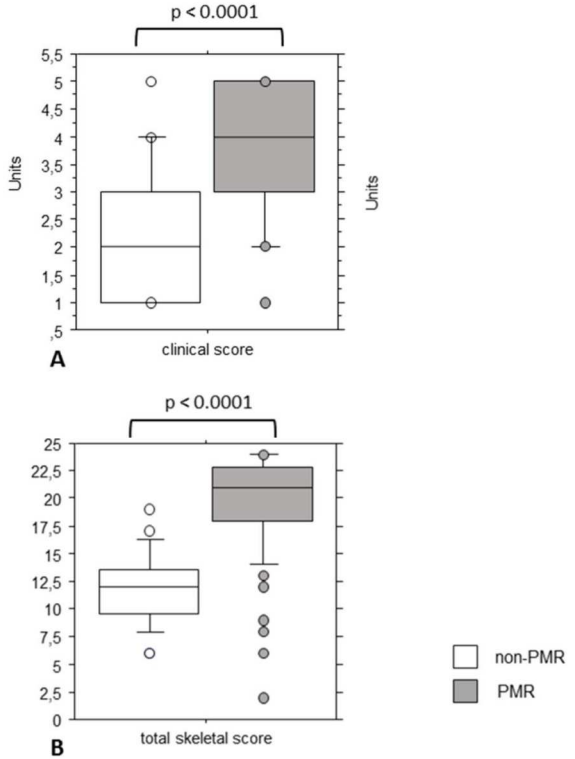

Figure 2. Clinical score (panel A) and total skeletal score (panel B) in PMR vs. non-PMR.

Rheumatology (Oxford). 2017 Oct 7. doi: 10.1093/rheumatology/kex376. [Epub ahead of print]

Use of 18F-fluorodeoxyglucose positron emission tomography in the diagnosis of polymyalgia rheumatica-A prospective study of 99 patients.

Henckaerts L, Gheysens O, Vanderschueren S, Goffin K, Blockmans D.

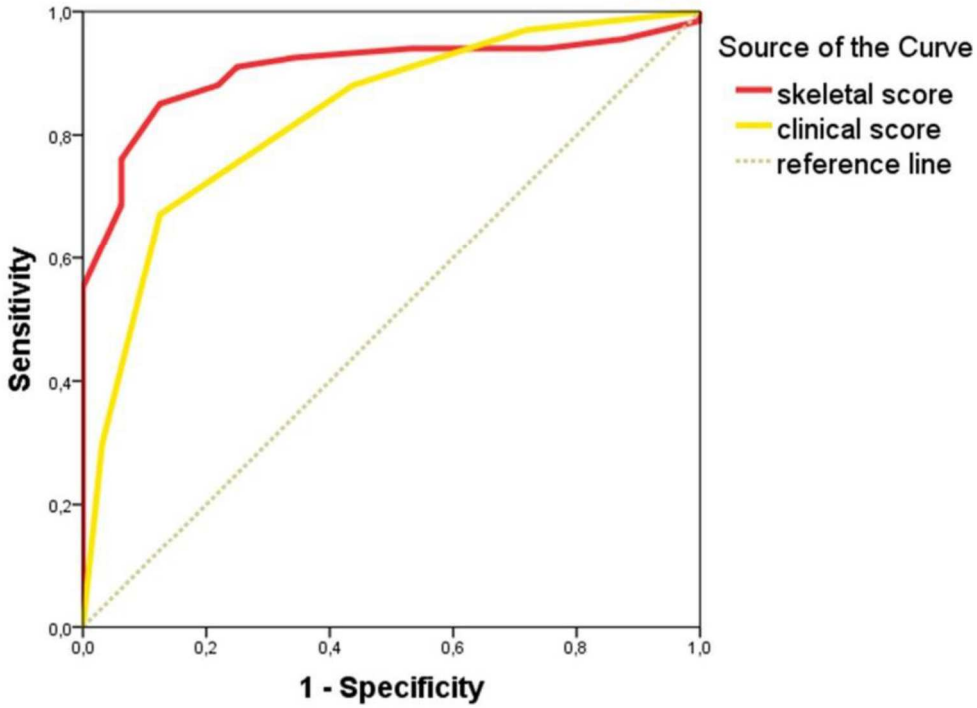

Figure 3. ROC-curve analysing the performance of the clinical score and the FDG-PET total skeletal score.

Rheumatology (Oxford). 2017 Oct 7. doi: 10.1093/rheumatology/kex376. [Epub ahead of print]

Use of 18F-fluorodeoxyglucose positron emission tomography in the diagnosis of polymyalgia rheumatica-A prospective study of 99 patients.

Henckaerts L, Gheysens O, Vanderschueren S, Goffin K, Blockmans D.

RESULTS

- 67 patients were diagnosed with PMR

- The median clinical score was 4 (IQR 3-5) in patients with PMR vs. 2 (IQR 1-3) in patients without PMR ($p<0.0001$) (figure 2).

In the ROC analysis the area under the curve (AUC) for the clinical score was 0.830 +/- 0.044 ($p<0.0001$) (figure 3). The ideal clinical score for differentiation between PMR and non-PMR was 4, with a sensitivity of 67.2 %, a specificity of 87.5 %, a PPV of 91.8 % and a NPV of 56.0%.

- The median total skeletal score was 21.0 (IQR 18.0-22.8) in patients with PMR as compared to 12.0 (IQR 9.5-13.5) in patients without PMR ($p<0.0001$) (figure 2).

In the ROC analysis the AUC for the total skeletal score was 0.905 +/- 0.031 ($p<0.0001$) (figure 3). The ideal total skeletal score for differentiation between PMR and non-PMR was 16, with a sensitivity of 85.1% and a specificity of 87.5% (PPV 93.4%, NPV 73.7%).

Rheumatology (Oxford). 2017 Oct 7. doi: 10.1093/rheumatology/kex376. [Epub ahead of print]

Use of 18F-fluorodeoxyglucose positron emission tomography in the diagnosis of polymyalgia rheumatica-A prospective study of 99 patients.

Henckaerts L, Gheysens O, Vanderschueren S, Goffin K, Blockmans D.

CONCLUSIONS

- FDG-PET before the start of treatment improves the diagnostic accuracy in suspected PMR.
- A total skeletal score of >16 has a sensitivity of 85.1% and a specificity of 87.5%.
- FDG-PET can therefore be a reliable aid in case of an atypical clinical picture.

Rheumatology (Oxford). 2017 Oct 7. doi: 10.1093/rheumatology/kex376. [Epub ahead of print]

EULAR recommendations for the use of imaging in large vessel vasculitis in clinical practice

Christian Dejaco,[1,2] Sofia Ramiro,[3] Christina Duftner,[4] Florent L Besson,[5,6] Thorsten A Bley,[7] Daniel Blockmans,[8] Elisabeth Brouwer,[9] Marco A Cimmino,[10] Eric Clark,[11] Bhaskar Dasgupta,[12,13] Andreas P Diamantopoulos,[14] Haner Direskeneli,[15] Annamaria Iagnocco,[16] Thorsten Klink,[7] Lorna Neill,[17] Cristina Ponte,[18,19] Carlo Salvarani,[20,21] Riemer H J A Slart,[22,23] Madeline Whitlock,[12] Wolfgang A Schmidt[24]

Dejaco C, et al. Ann Rheum Dis 2018;**0**:1–8. doi:10.1136/annrheumdis-2017-212649

EULAR recommendations for the use of imaging in large vessel vasculitis in clinical practice.

Dejaco C, Ramiro S, Duftner C, Besson FL, Bley TA, Blockmans D, Brouwer E, Cimmino MA, Clark E, Dasgupta B, Diamantopoulos AP, Direskeneli H, Iagnocco A, Klink T, Neill L, Ponte C, Salvarani C, Slart RHJA, Whitlock M, Schmidt WA.

Table 2 EULAR recommendations for the use of imaging in LVV in clinical practice

Statement	LoE	LoA
1. In patients with suspected GCA, an early imaging test is recommended to complement the clinical criteria for diagnosing GCA, assuming high expertise and prompt availability of the imaging technique. Imaging should not delay initiation of treatment.	1	9.2 (2.1) 90% ≥8
2. In patients in whom there is a high clinical suspicion of GCA and a positive imaging test, the diagnosis of GCA may be made without an additional test (biopsy or further imaging). In patients with a low clinical probability and a negative imaging result, the diagnosis of GCA can be considered unlikely. In all other situations, additional efforts towards a diagnosis are necessary.	2	9.4 (1.0) 90% ≥8
3. Ultrasound of temporal±axillary arteries is recommended as the first imaging modality in patients with suspected predominantly cranial GCA*. A non-compressible 'halo' sign is the ultrasound finding most suggestive of GCA.	1	9.7 (0.6) 100% ≥8
4. High resolution MRI† of cranial arteries‡ to investigate mural inflammation may be used as an alternative for GCA diagnosis if ultrasound is not available or inconclusive.	2	9.2 (1.1) 90% >8
5. CT† and PET† are not recommended for the assessment of inflammation of cranial arteries.	5	9.5 (1.2) 95% >8
6. Ultrasound, PET, MRI and/or CT may be used for detection of mural inflammation and/or luminal changes in extracranial arteries to support the diagnosis of LV-GCA. Ultrasound is of limited value for assessment of aortitis.	3 (PET and CT) and 5 (MRI and ultrasound)	9.8 (0.6) 100% ≥8
7. In patients with suspected TAK, MRI to investigate mural inflammation and/or luminal changes should be used as the first imaging test to make a diagnosis of TAK, assuming high expertise and prompt availability of the technique.	3	9.1 (1.4) 90% >8
8. PET, CT and/or ultrasound may be used as alternative imaging modalities in patients with suspected TAK. Ultrasound is of limited value for assessment of the thoracic aorta.	3 (CT) and 5 (PET and ultrasound)	9.4 (0.8) 100% ≥8
9. Conventional angiography is not recommended for the diagnosis of GCA or TAK as it has been superseded by the previously mentioned imaging modalities.	5	9.8 (0.6) 100% ≥8
10. In patients with LVV (GCA or TAK) in whom a flare is suspected, imaging might be helpful to confirm or exclude it. Imaging is not routinely recommended for patients in clinical and biochemical remission.	5	9.4 (0.8) 100% ≥8
11. In patients with LVV (GCA or TAK), MRA, CTA and/or ultrasound may be used for long-term monitoring of structural damage, particularly to detect stenosis, occlusion, dilatation and/or aneurysms. The frequency of screening as well as the imaging method applied should be decided on an individual basis.	5	9.3 (1.2) 95% ≥8
12. Imaging examination should be done by a trained specialist using appropriate equipment, operational procedures and settings. The reliability of imaging, which has often been a concern, can be improved by specific training. Suggestions for technical and operational parameters are depicted in box 1.	5	9.8 (0.6) 100% ≥8

Ann Rheum Dis. 2018 Jan 22. pii: annrheumdis-2017-212649

[^{18}F]-Fluorodeoxyglucose (FDG) positron emission tomography (PET)

- Hybrid PET with low-dose CT.
- Blood glucose levels: preferred <7 mmol/L (126 mg/dL), <10 mmol/L (180 mg/dL) acceptable.
- Interval between FDG infusion and image acquisition should be at least 60 min, preferably 90 min.
- Position of patient is supine, position of the arms should be arms down.
- Body parts to include: from top of head to at least midthigh, preferably to below the knees.
- Scoring FDG uptake: qualitative visual grading; if result is unclear, compare it with the liver background (grading 0–3).

New treatments in GCA

(besides steroids and methotrexate)

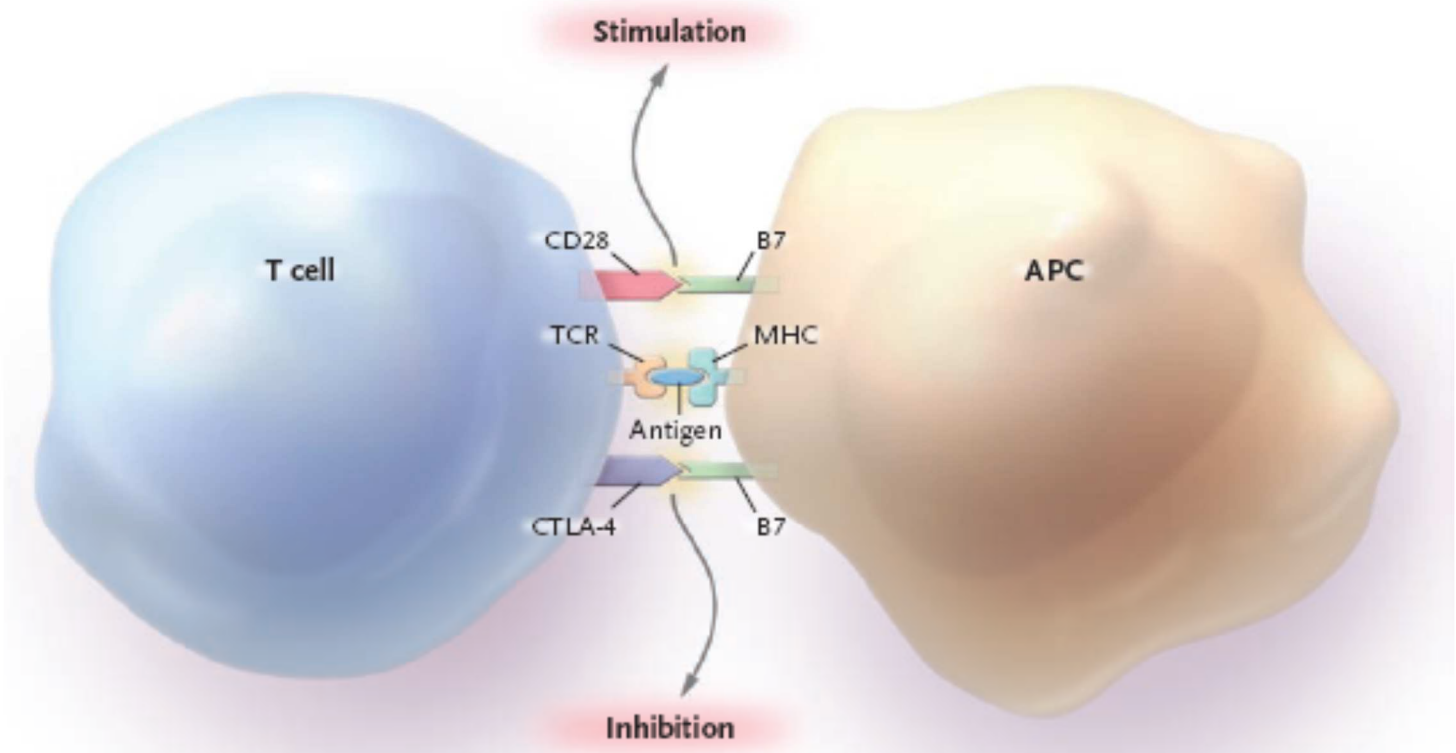

Figure 1. Interaction between a T Cell and an Antigen-Presenting Cell (APC).

The antigen-presenting cell binds antigen in a complex with a molecule from the major histocompatibility complex (MHC) on its surface. This complex interacts with the T-cell receptor (TCR). The effect on the T cell depends on the interaction between other molecules on the surfaces of the two cells. Two alternative interactions are shown: B7 with CD28, which is stimulatory, and B7 with cytotoxic T-lymphocyte–associated protein 4 (CTLA-4), which is inhibitory. If the positive signal caused by the CD28–B7 interaction dominates, the T cell is activated, leading to cytokine release, B-cell help, and inflammation. If the negative signal caused by the CTLA-4–B7 interaction dominates, activation is suppressed.

N Engl J Med 2008; 358: 929-939.

Drug-associated polymyalgia rheumatica/giant cell arteritis occurring in two patients after treatment with ipilimumab, an antagonist of CTLA-4.

Goldstein BL, Gedmintas L, Todd DJ.

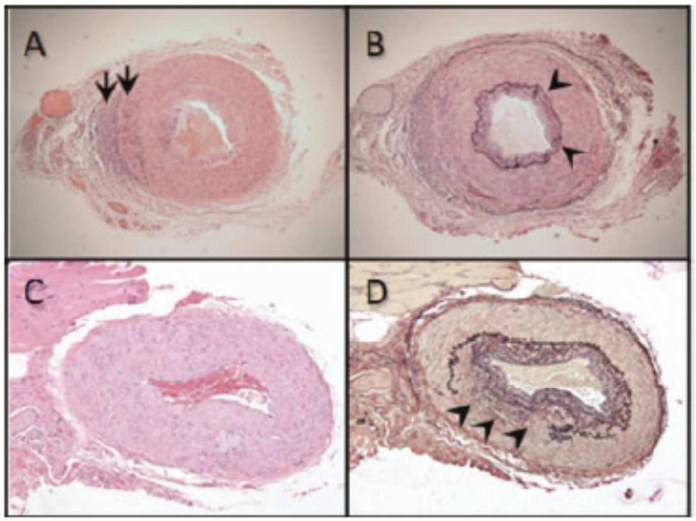

Figure 1. A and **B,** Histologic findings in case 1. **A,** Temporal artery biopsy showing an inflammatory infiltrate in the adventitia and muscularis layers (**arrows**) and narrowing of the lumen, consistent with intimal proliferation and active arteritis. **B,** Elastin staining showing early, small focal disruptions of the internal elastic lamina (**arrowheads**). **C** and **D,** Histologic findings in case 1. **C,** Temporal artery biopsy showing healed arteritis with intimal proliferation. **D,** Elastin staining showing disruption of the internal elastic lamina (**arrowheads**). Original magnification × 100.

Arthritis Rheumatol 2014; 66:768-9.

A randomized, double-blind trial of abatacept (CTLA4-IG) for the treatment of giant cell arteritis

Carol A. Langford MD MHS ✉, David Cuthbertson MS, Steven R. Ytterberg MD, Nader Khalidi MD, Paul A. Monach MD PhD, Simon Carette MD, Philip Seo MD MHS, Larry W. Moreland MD, Michael Weisman MD, Curry L Koening MD, Antoine Sreih MD, Robert Spiera MD, Carol A. McAlear MA, Kenneth J. Warrington MD, Christian Pagnoux MD, Kathleen McKinnon DO, Lindsy J. Forbess MD, Gary S. Hoffman MD MS, Renée Borchin, Jeffrey P. Krischer PhD, Peter A. Merkel MD MPH, for the Vasculitis Clinical Research Consortium

Langford C, et al. Arthritis Rheum 2017; 69: 837-45

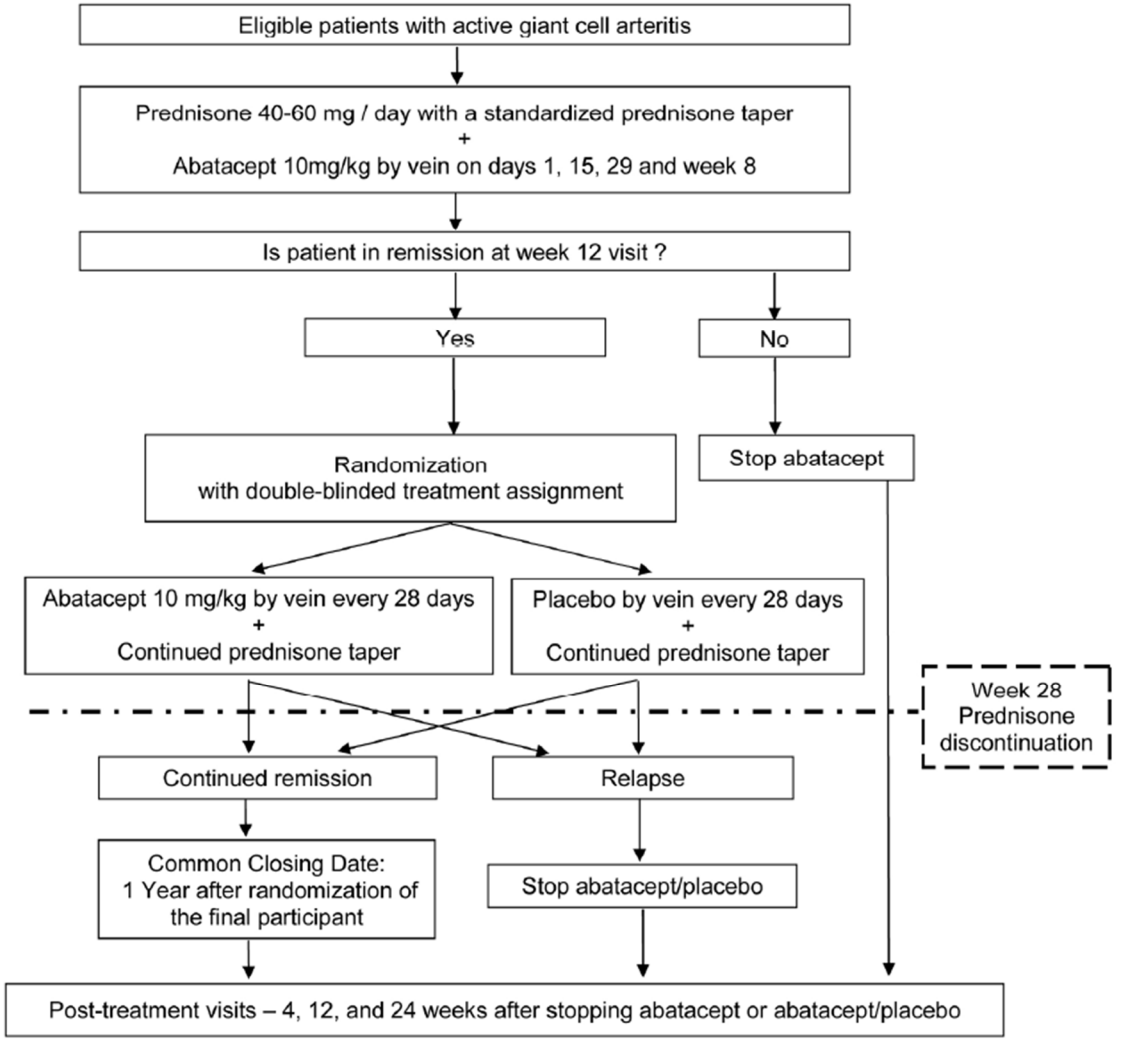

Langford C, et al. Arthritis Rheum 2017; 69: 837-45

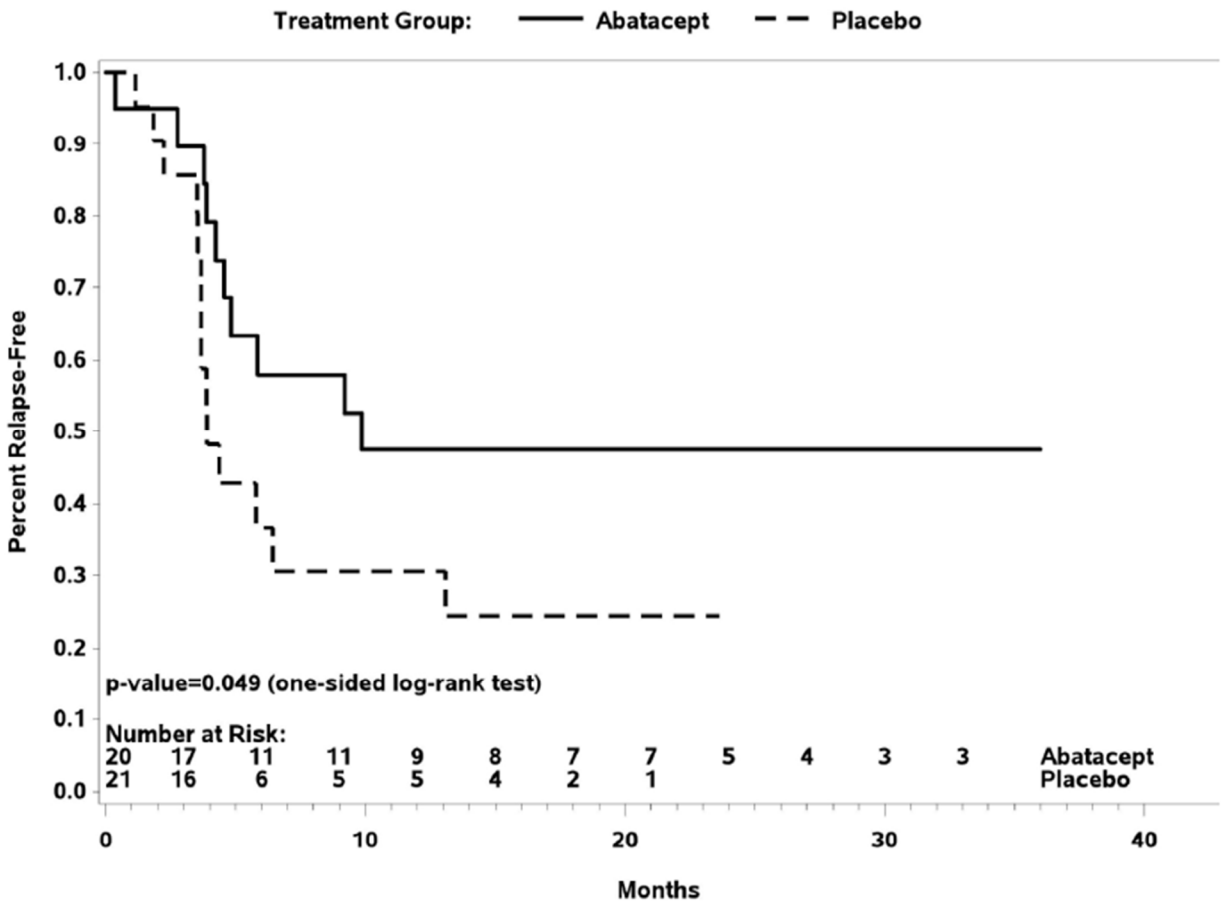

Langford C, et al. Arthritis Rheum 2017; 69: 837-45

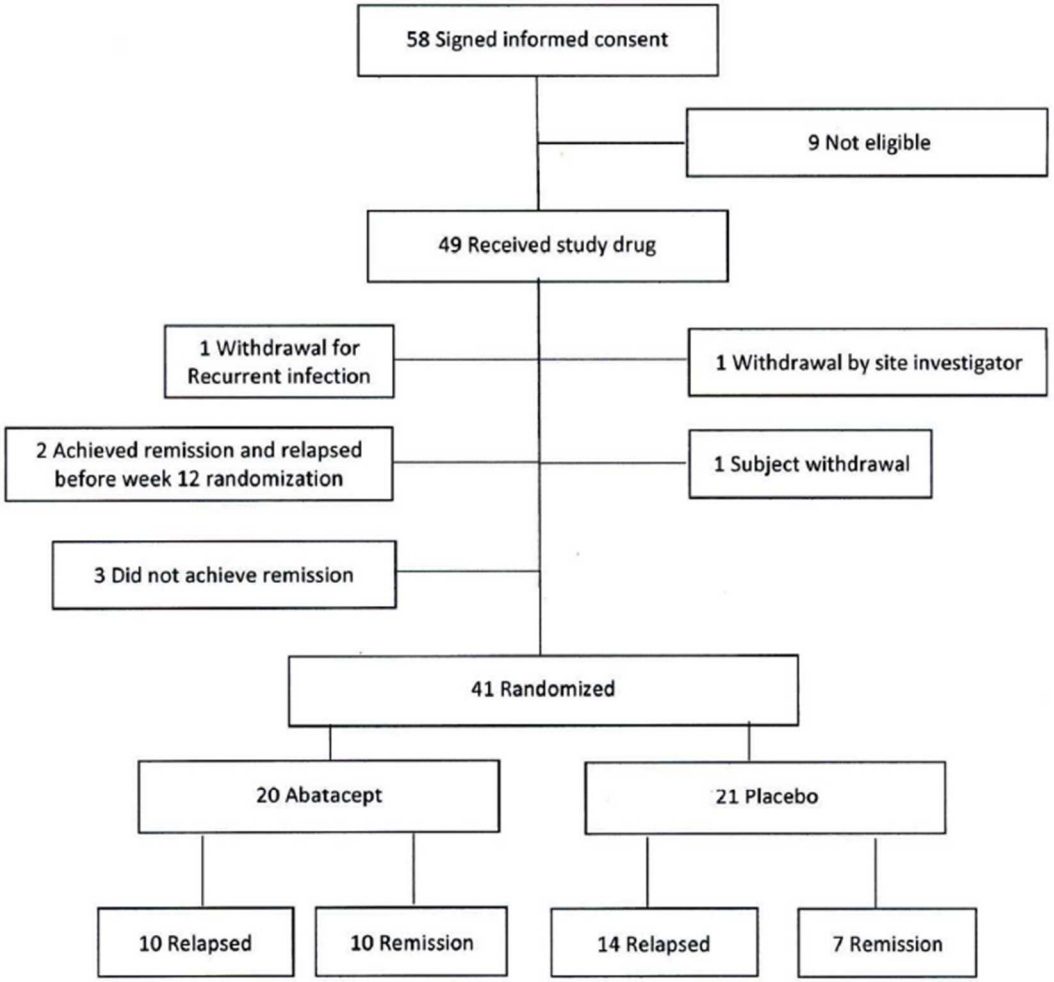

Langford C, et al. Arthritis Rheum 2017; 69: 837-45

Role of interleukin-6 in giant cell arteritis

- IL-6 is secreted by numerous immune cells, including macrophages, neutrophils, dendritic cells, and CD4T cells
- IL-6 has an effect on the activation of neutrophils and macrophages, the differentiation of T-helper cells into type 17 T-helper cells (Th17 cells), the inhibition of T-regulatory cells, the promotion and differentiation of B cells, and the stimulation of endothelial cells
- IL-6 potently stimulates hepatocytes to release the acute-phase proteins

Roberts J, Clifford A. Ther Adv Chronic Dis 2017; 8: 69-79

Tocilizumab for induction and maintenance of remission in giant cell arteritis: a phase 2, randomised, double-blind, placebo-controlled trial

Villiger P, Adler S, Kuchen S, Wermelinger F, Dan D, Fiege V, Bütikofer L, Seitz M, Reichenbach S

Results

Between March 3, 2012, and Sept 9, 2014, 20 patients were randomly assigned to receive tocilizumab and prednisolone, and ten patients to receive placebo and glucocorticoid; 16 (80%) and seven (70%) patients, respectively, had new-onset giant cell arteritis. 17 (85%) of 20 patients given tocilizumab and four (40%) of ten patients given placebo reached complete remission by week 12 (risk difference 45%, 95% CI 11–79; p=0·0301). Relapse-free survival was achieved in 17 (85%) patients in the tocilizumab group and two (20%) in the placebo group by week 52 (risk difference 65%, 95% CI 36–94; p=0·0010). The mean survival-time difference to stop glucocorticoids was 12 weeks in favour of tocilizumab (95% CI 7–17; p<0·0001), leading to a cumulative prednisolone dose of 43 mg/kg in the tocilizumab group versus 110 mg/kg in the placebo group (p=0·0005) after 52 weeks. Seven (35%) patients in the tocilizumab group and five (50%) in the placebo group had serious adverse events.

Interpretation

Our findings show, for the first time in a trial setting, the efficacy of tocilizumab in the induction and maintenance of remission in patients with giant cell arteritis.

Lancet 2016; 387: 1921-1927

Tocilizumab for induction and maintenance of remission in giant cell arteritis: a phase 2, randomised, double-blind, placebo-controlled trial

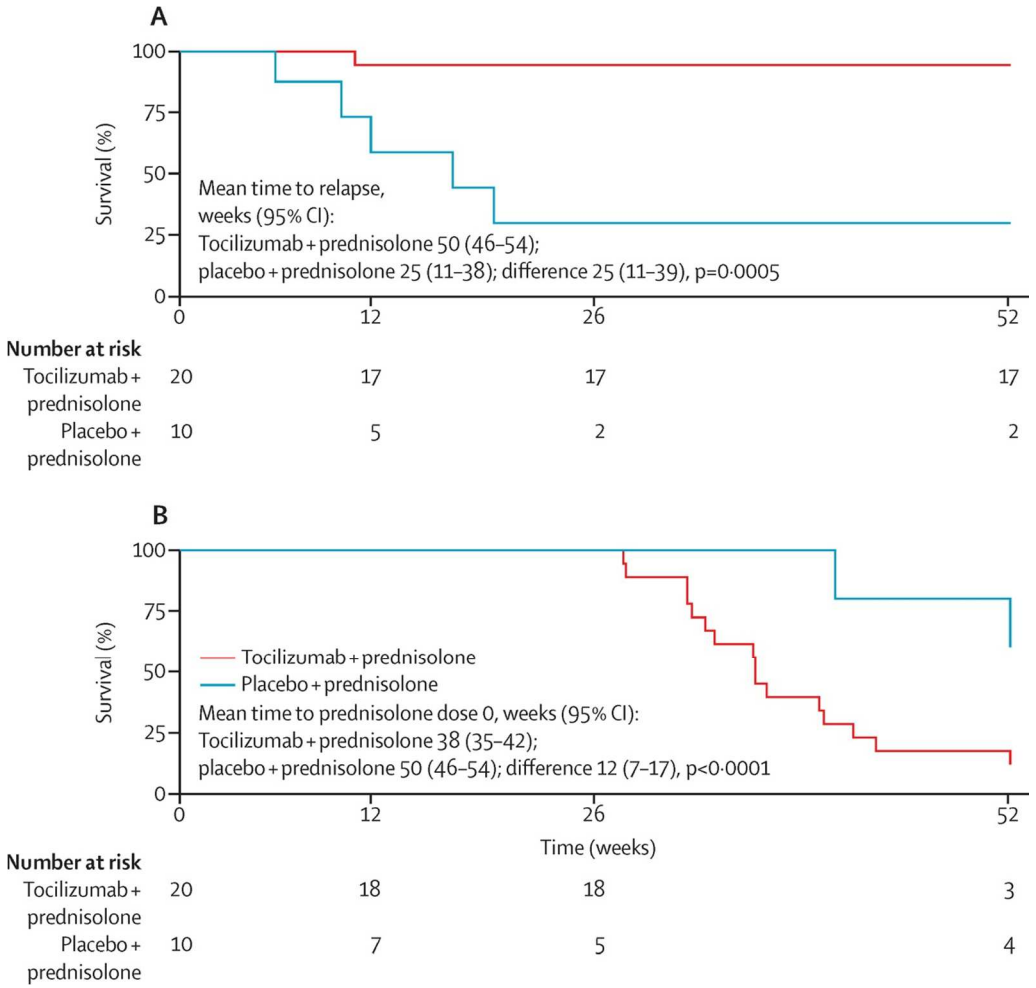

The Lancet 2016;387:1921-7

The GiACTA Trial
Tocilizumab for Sustained Glucocorticoid-Free Remission in Giant Cell Arteritis

John H. Stone,[1] Katie Tuckwell,[2] Sophie Dimonaco,[2] Micki Klearman,[3] Martin Aringer,[4] Daniel Blockmans,[5] Elisabeth Brouwer,[6] Maria C. Cid,[7] Bhaskar Dasgupta,[8] Juergen Rech,[9] Carlo Salvarani,[10] Robert Spiera,[11] Sebastian H. Unizony,[1] the GiACTA Investigators, and Neil Collinson[2]

[1]Harvard Medical School, Boston, MA, USA; [2]Roche Products Ltd., Welwyn Garden City, UK; [3]Genentech, South San Francisco, CA, USA; [4]Abteilung für Rheumatologie, Dresden, Germany; [5]University Hospitals Gasthuisberg, Leuven, Belgium; [6]University of Groningen, Groningen, Netherlands; [7]University of Barcelona, Barcelona, Spain; [8]Southend University Hospital, NHS Foundation Trust, Westcliff-on-Sea, UK; [9]Friedrich-Alexander-University Erlangen-Nürnberg, Germany; [10]Arcispedale Santa Maria Nuova-IRCCS, Reggio Emilia, Italy; [11]Hospital for Special Surgery, Cornell, NY, USA

New Engl J Med 2017; 377: 317-328

Methods

- **Central hypothesis:**
  TCZ has a powerful steroid-sparing effect
- **First trial (in any disease): a blinded, variable-dose steroid regimen**
  - **Prednisone doses <20 mg/day were double-blind**
- **Dual-assessor approach**
  - **ALL investigators blinded to CRP**
- **Enrolled 251 patients over 22 months**
- **14 countries, 76 sites (61 Europe, 15 North America)**

Eligibility Criteria:
Modified 1990 ACR Classification Criteria

- **Age at onset >50 years**
- **ESR >50 mm/h (or CRP ≥2.45 mg/dL)**

- **Unequivocal cranial symptoms of GCA and/or**
- **Unequivocal symptoms of PMR**

- **Temporal artery biopsy and/or**
- **Imaging evidence of large-vessel vasculitis**

Four Groups

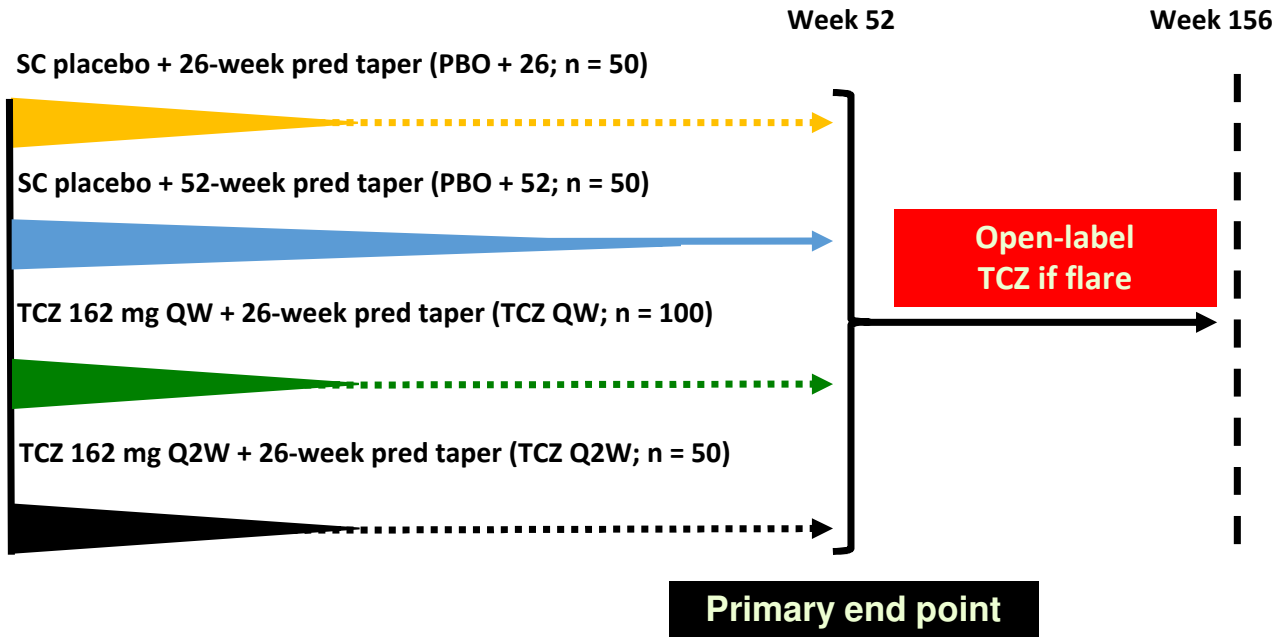

PBO, placebo; pred, prednisone; Q2W, once every 2 weeks; QW, once a week; SC, subcutaneous.

Definitions

- **Flare: determined by the investigator and defined as the recurrence of signs or symptoms of GCA and/or ESR ≥30 mm/h attributable to GCA**
  - **An increase in the prednisone dose was required**
- **Remission: absence of flare and normalization of the CRP (<1 mg/dL)**
  - **A single CRP elevation (≥1 mg/dL) not considered absence of remission unless CRP remained elevated (≥1 mg/dL) at the next study visit**
- **Sustained remission: absence of flare following induction of remission within 12 weeks of BL and maintained up to week 52**

BL, baseline.

End Points

- **Primary end point**
  - **TCZ + 26-week prednisone versus 26-week prednisone only: sustained remission from week 12 to week 52 AND adherence to the protocol-defined prednisone taper**
- **Key secondary end point**
  - **TCZ + 26-week prednisone versus 52-week prednisone: sustained remission from week 12 to week 52 AND adherence to the protocol-defined prednisone taper**
- **Other secondary end points**
  - **Time to flare**
  - **Cumulative glucocorticoid use**
  - **Quality of life**
- **Safety**

Results

Baseline Characteristics	All Patients N = 251
Age, mean (SD)	69.0 (8.2)
Female, %	74.9
Caucasian, %	96.8
Newly diagnosed, %	47.4
Relapsing, %	52.6

SD, standard deviation.

Sustained Remission: Primary and Key Secondary End Points

- Superior efficacy of TCZ + 26-week prednisone versus 26-week and 52-week prednisone alone

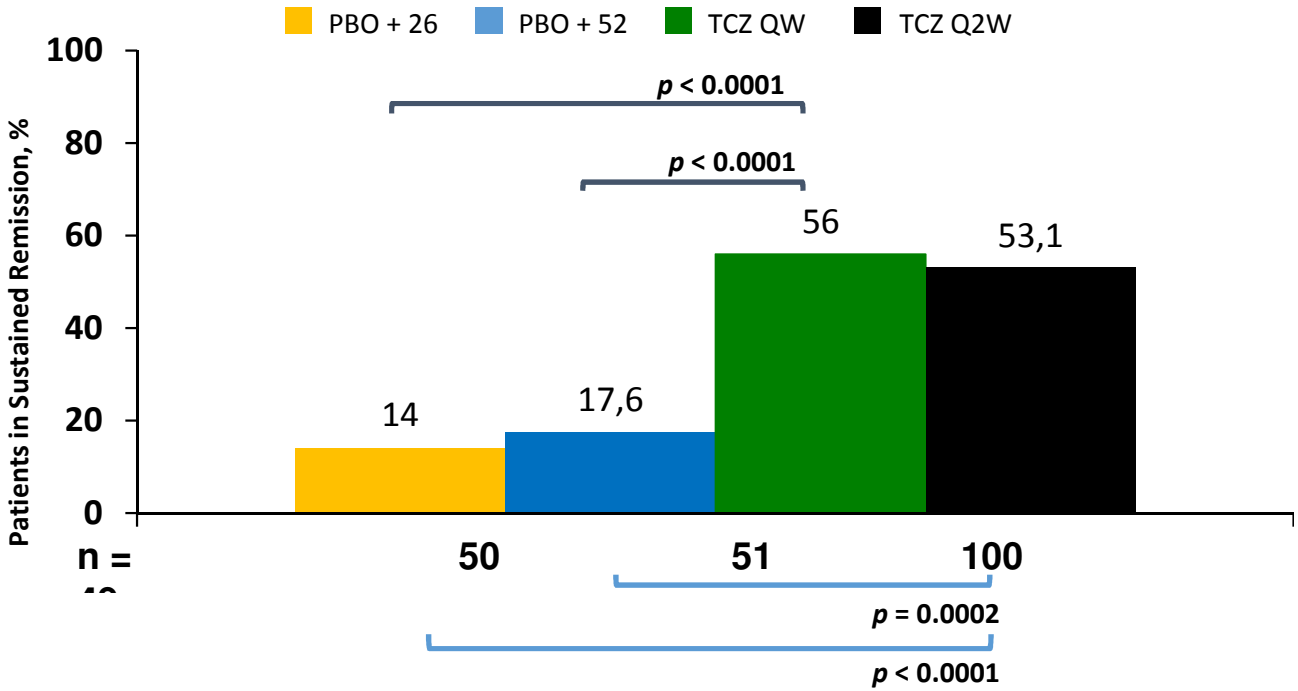

Sustained remission: New onset and relapsing patients

- Robust efficacy in new onset and relapsing pts supports a broad label
- QW efficacy numerically higher than Q2W across sub-groups

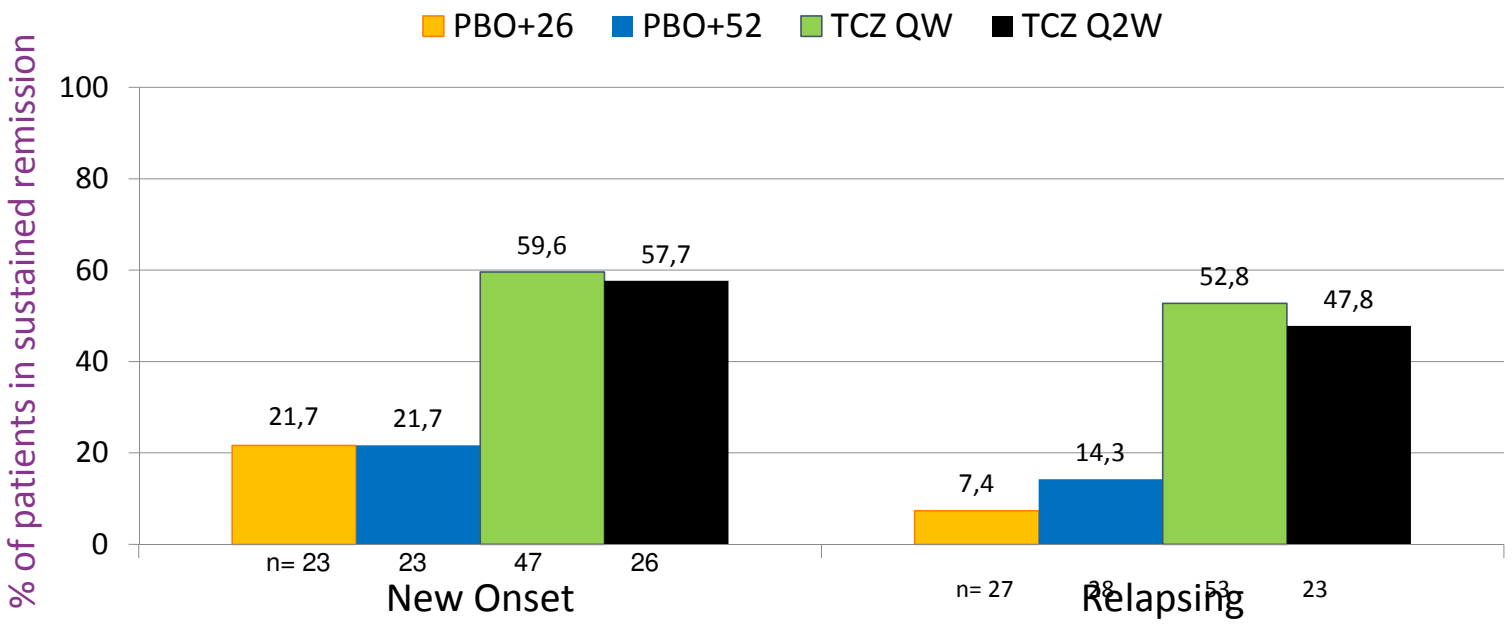

Sensitivity Analysis

Excluding CRP from the definition of sustained remission did not alter the conclusion of the primary analysis

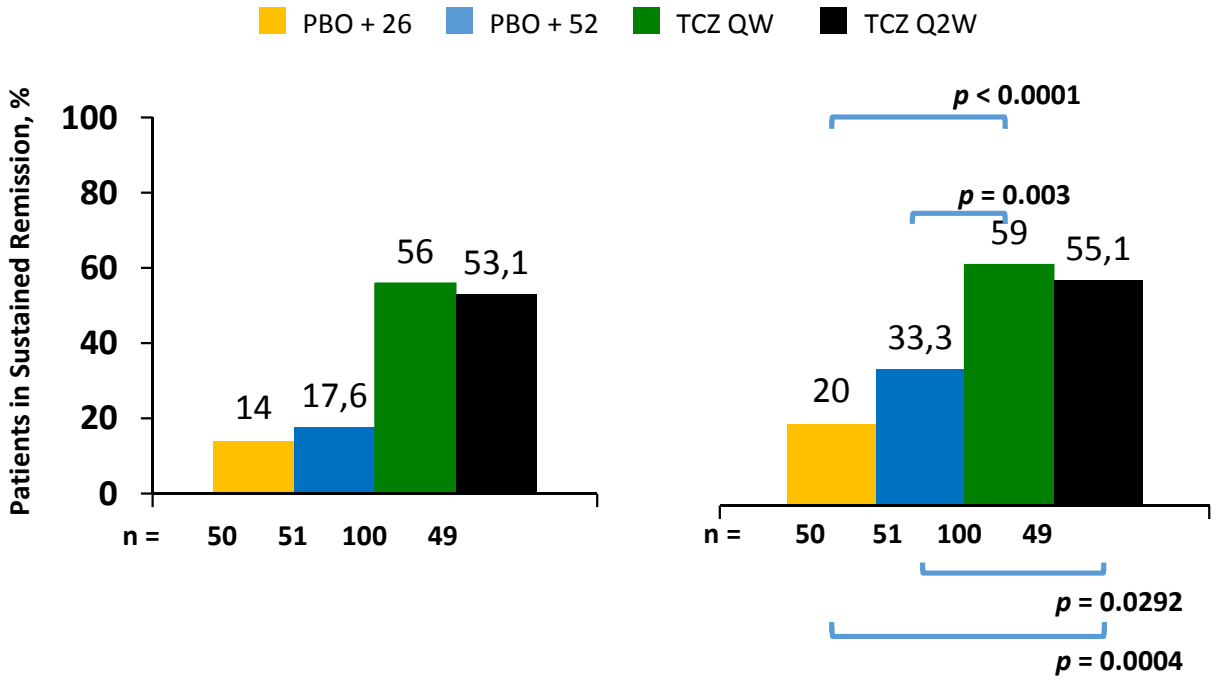

Time to First Flare Following Clinical Remission

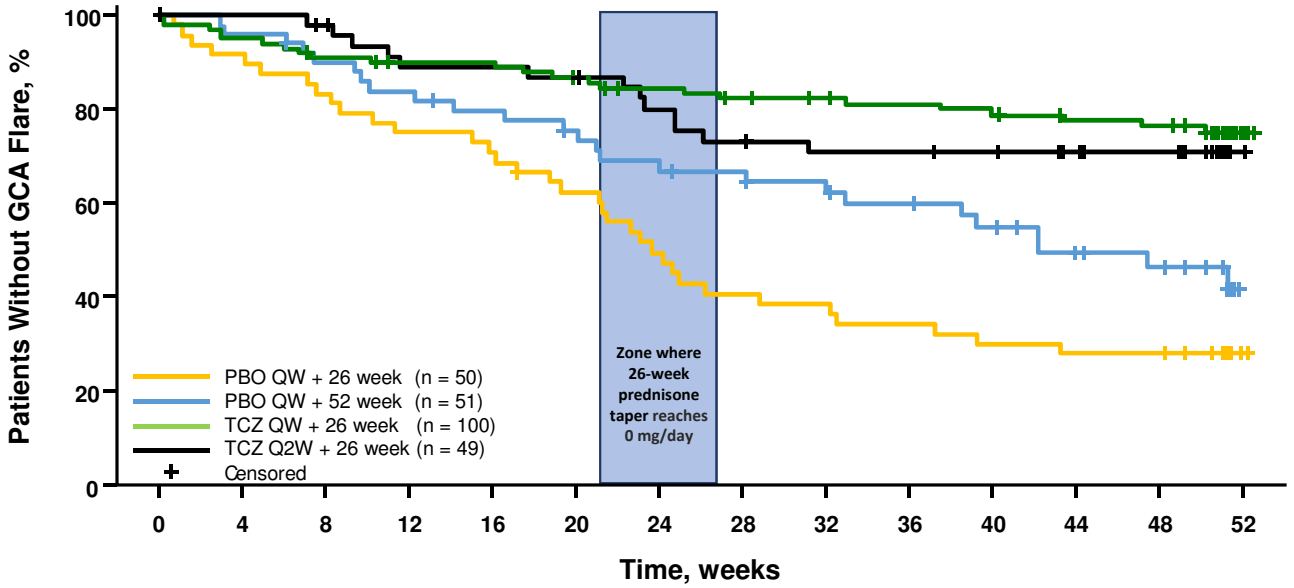

Time to first flare– new onset patients

- Clear differentiation between TCZ and steroid-only groups
- Time to first flare significantly longer for TCZ groups (vs PBO+26) only)

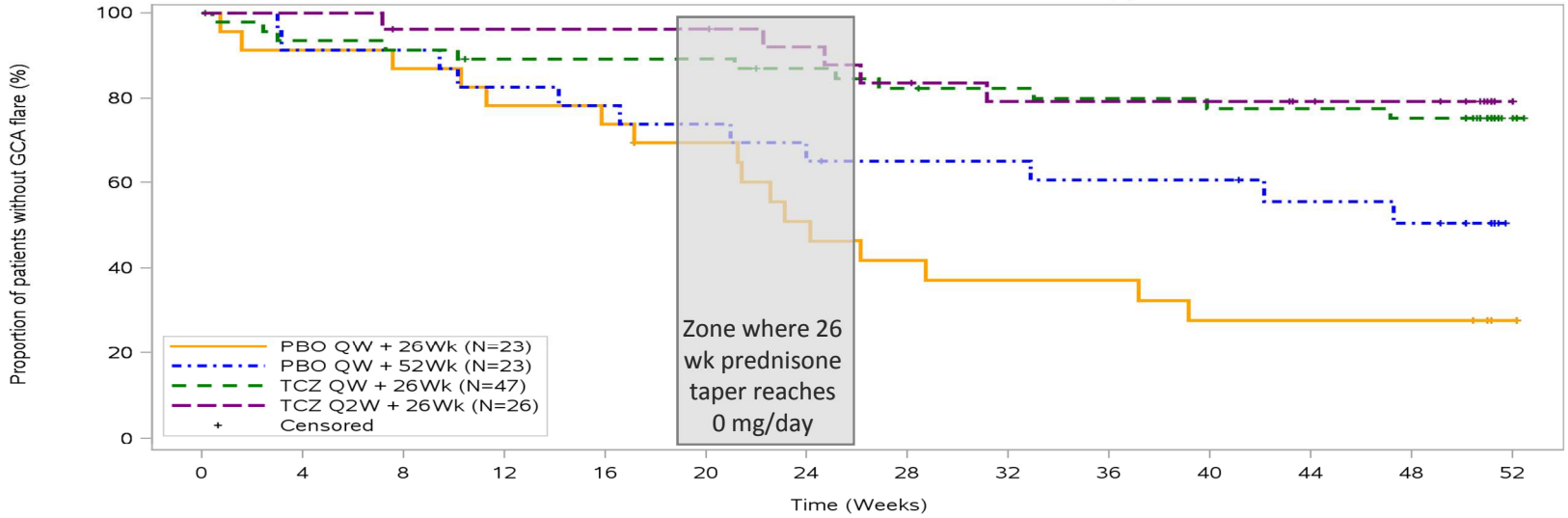

	Flare hazard ratio * p< 0.01	
Comparator	TCZ QW	TCZ Q2W
PBO + 26	0.25*	0.20*
PBO + 52	0.44	0.35

Time to first flare– relapsing patients

- Time to first flare significantly longer for TCZ groups
- Suggestion that Q2W does worse than QW in relapsing patients

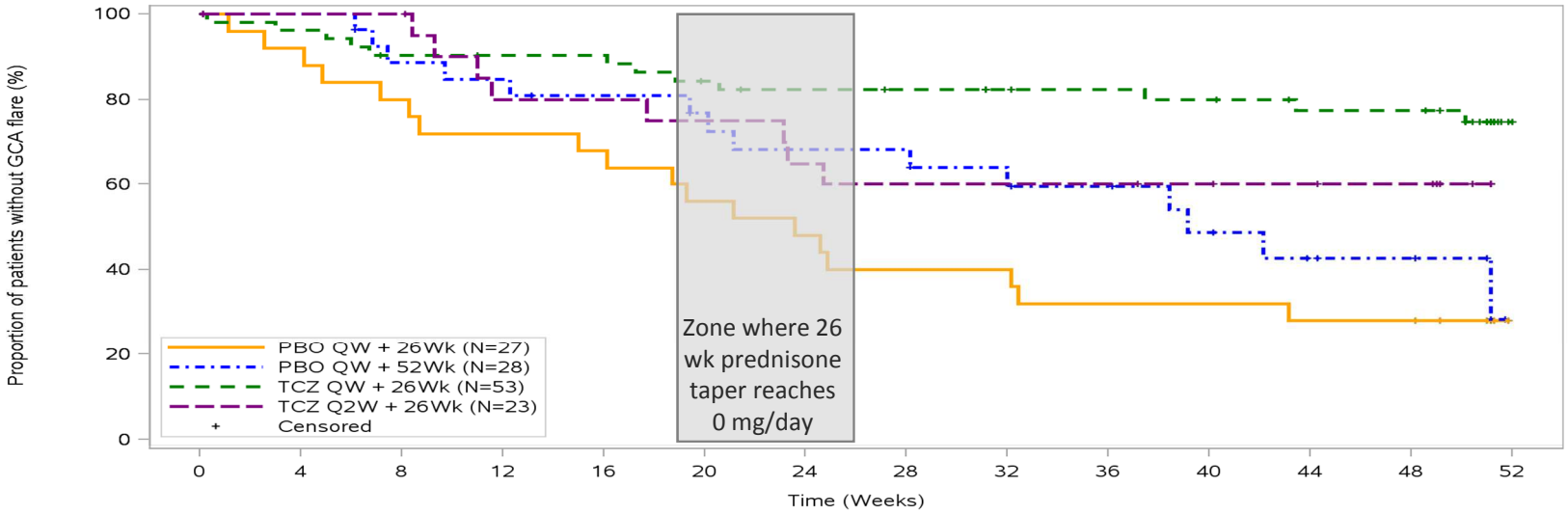

	Flare hazard ratio * p< 0.01	
Comparator	TCZ QW	TCZ Q2W
PBO + 26	0.23*	0.42*
PBO + 52	0.36*	0.67

TCZ Had a Significant Steroid-Sparing Effect

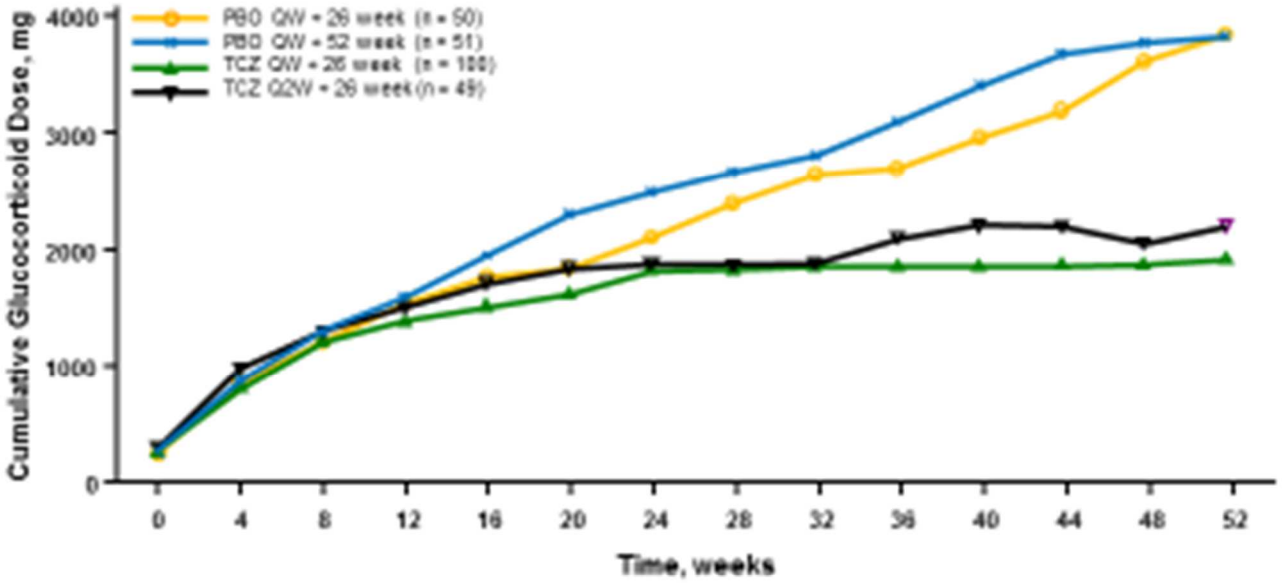

Actual Cumulative Dose to Week 52, mg	PBO + 26 n = 50	PBO + 52 n = 51	TCZ QW n = 100	TCZ Q2W n = 49
Median	**3296**	**3818**	**1862**	**1862**

Includes prednisone received as part of the taper, escape prednisone, and concomitant steroids.
$p < 0.0003$ for all comparisons of TCZ to PBO.

Safety Overview

- **AEs balanced across groups**
- **No new safety signals/laboratory abnormalities observed**
- **No deaths**
- **No bowel perforations**
- **2 malignancies (both in prednisone-only groups)**

	PBO + 26 n = 50	PBO + 52 n = 51	TCZ QW n = 100	TCZ Q2W n = 49
Pts with ≥1 AE, %	96.0	92.2	98.0	95.9
Total AEs, n	470	486	810	432
Pts with ≥1 SAE, %	22.0	25.5	15.0	14.3
Pts with ≥1 SI, %	4.0	11.8	7.0	4.1

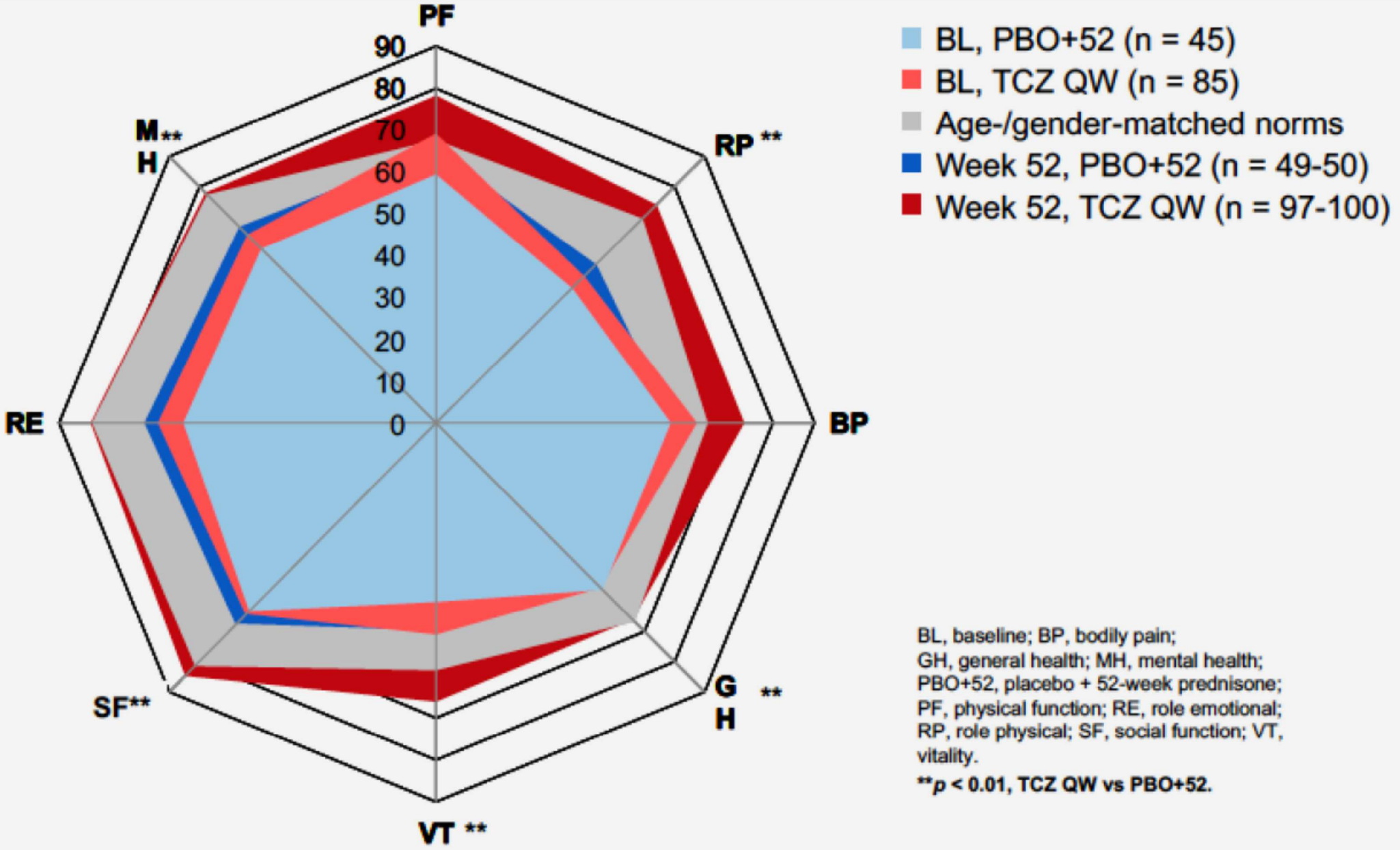

BL, baseline; BP, bodily pain; GH, general health; MH, mental health; PBO+52, placebo + 52-week prednisone; PF, physical function; RE, role emotional; RP, role physical; SF, social function; VT, vitality.

**$p < 0.01$, TCZ QW vs PBO+52.

What happens after tocilizumab is stopped ?

Termination of Tocilizumab-Treatment in Giant Cell Arteritis: Follow-up of Patients after the RCT (ClinicalTrials.gov registration number: NCT01450137)

Sabine Adler[1], Stephan Reichenbach[2], Stefan Kuchen[3], Felix Wermelinger[4], Diana Dan[4], Michael Seitz[4] and Peter M. Villiger[4], [1]Rheumatology, Immunology, Allergology, University Hospital Bern, Bern, Switzerland, [2]Institute of Social and Preventive Medicine, University of Bern, Bern, Switzerland, [3]Rheumatology, Immunology, and Allergology, University of Bern, Bern, MD, Switzerland, [4]Department of Rheumatology, Immunology and Allergology, University Hospital Bern, Bern, Switzerland

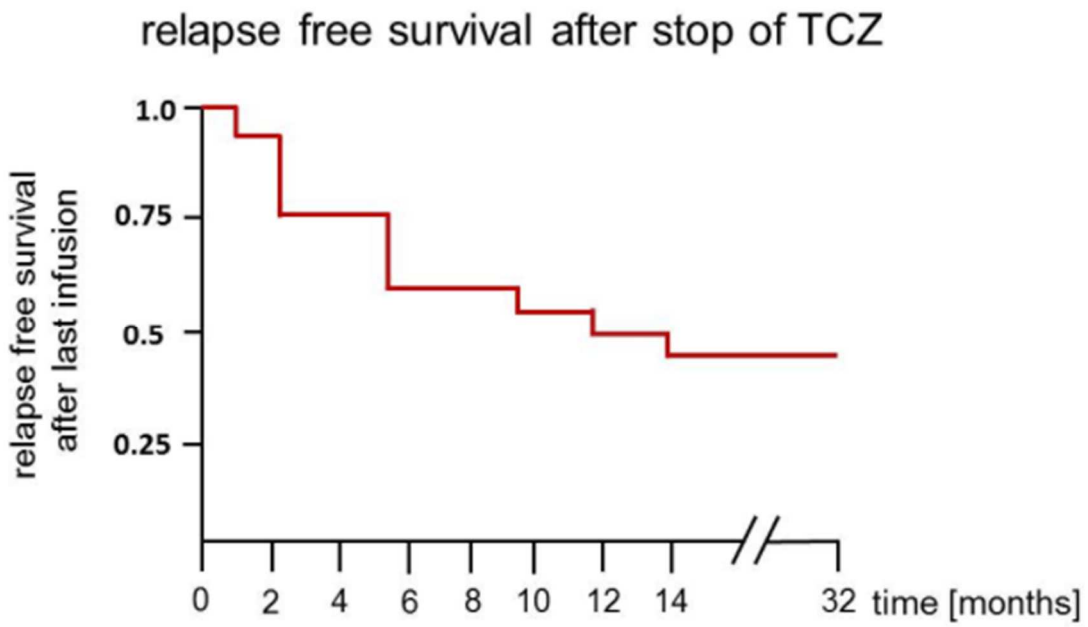

Arthritis Rheumatol. 2016; 68 (suppl 10)

What happens after tocilizumab is stopped ?

- Last patient will end 2-year follow-up period June 2018, results probably available by end 2018
- Leuven : inclusion of 13 patients in Giacta trial (last patient will end follow-up in April 2018) : 10/13 did a relapse during this 2-year follow-up, a mean of 13 ± 5 months (6-19 months) after the end of phase 1

Sirresta – study

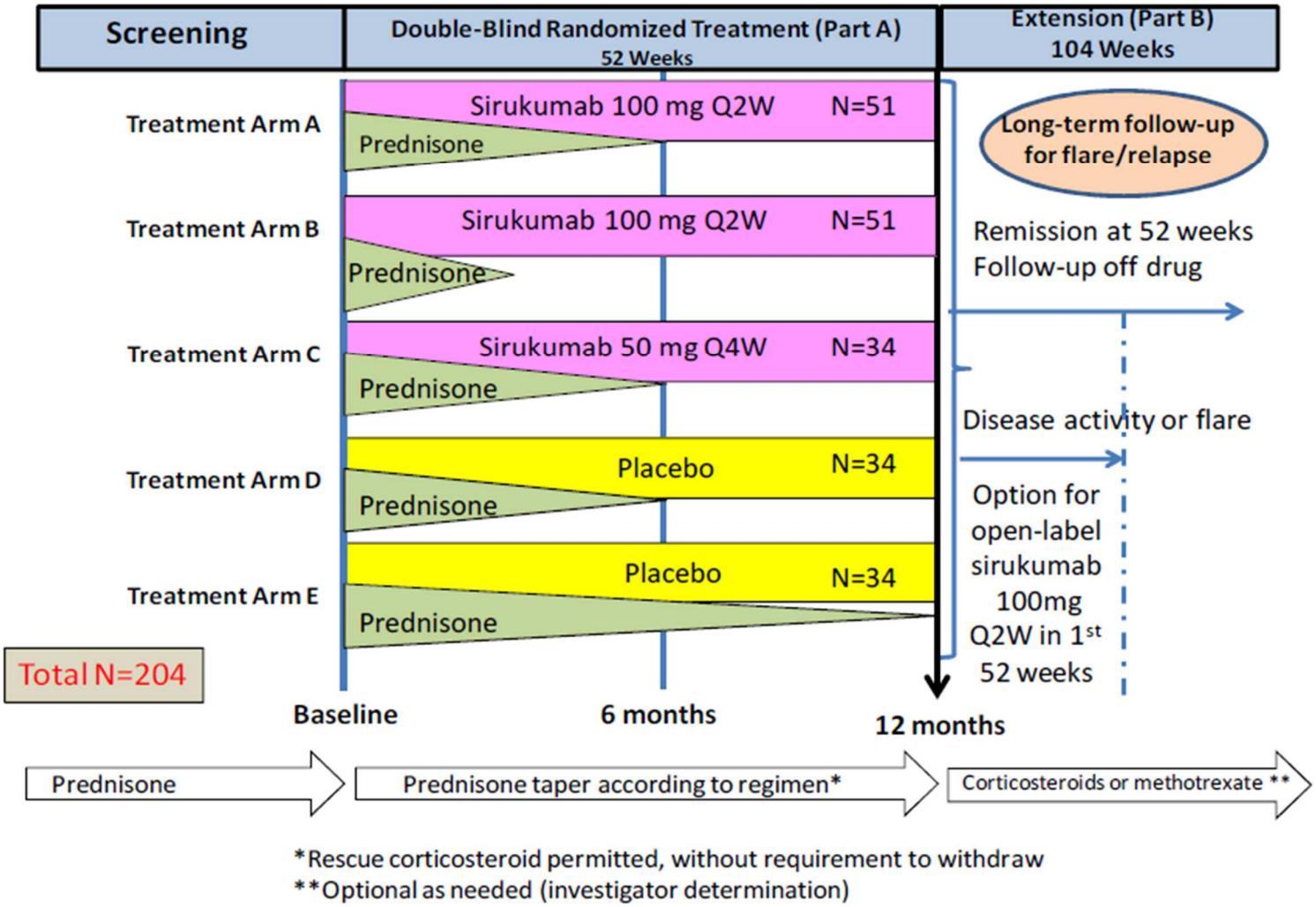

*Rescue corticosteroid permitted, without requirement to withdraw
**Optional as needed (investigator determination)

Tocilizumab for the treatment of large-vessel vasculitis (giant cell arteritis, Takayasu arteritis) and polymyalgia rheumatica.

Unizony S, Arias-Urdaneta L, Miloslavsky E, Arvikar S, Khosroshahi A, Keroack B, Stone JR, Stone JH.

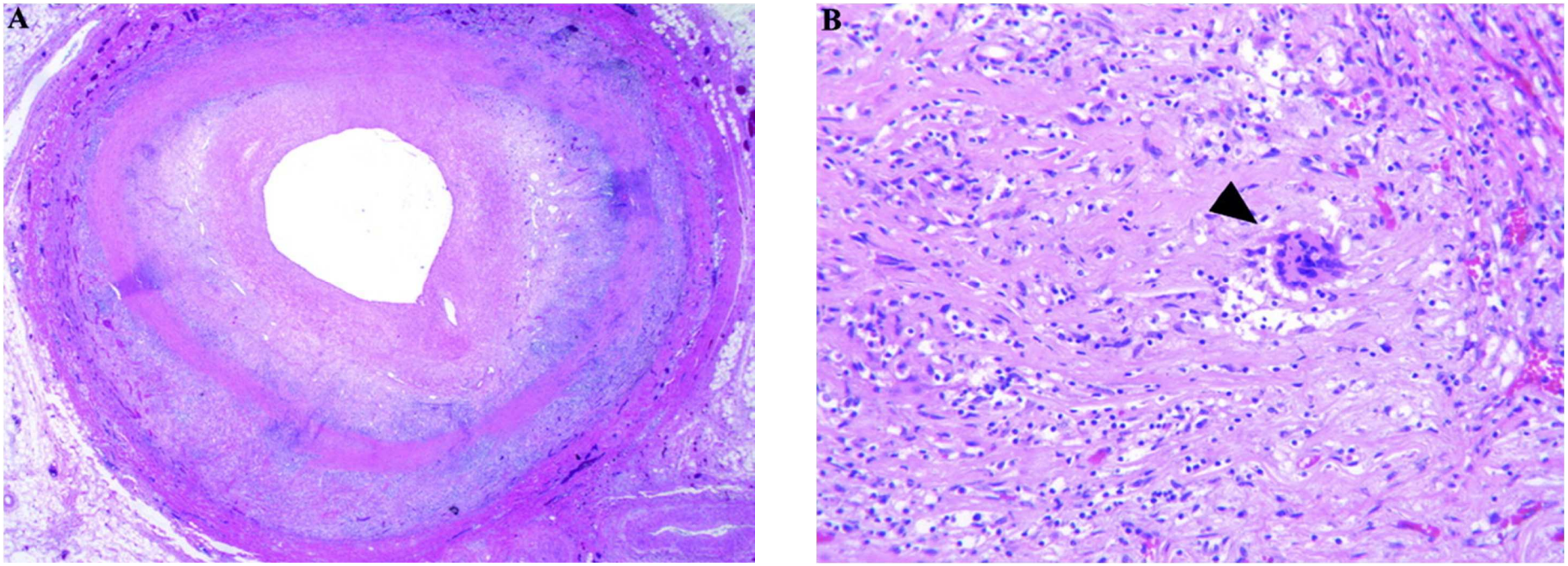

Persistent vasculitis in one patient at autopsy who died of a postoperative myocardial infarction. A, Right subclavian artery at autopsy. A low-power image of the right subclavian artery shows active vasculitis with extensive inflammation in the media and with intimal hyperplasia and narrowing of the lumen. B, Right subclavian artery at autopsy. A high-power histologic image of the right subclavian artery shows extensive inflammatory infiltration of the media with necrosis and giant cell formation (arrow head) indicative of active giant cell arteritis.

Arthritis Care Res (Hoboken). 2012; 64: 1720-9.

Magnetic resonance angiography in giant cell arteritis: results of a randomized controlled trial of tocilizumab in giant cell arteritis

Fig. 1 Percentages of patients with vasculitis at different locations at baseline, 12 and 52 weeks

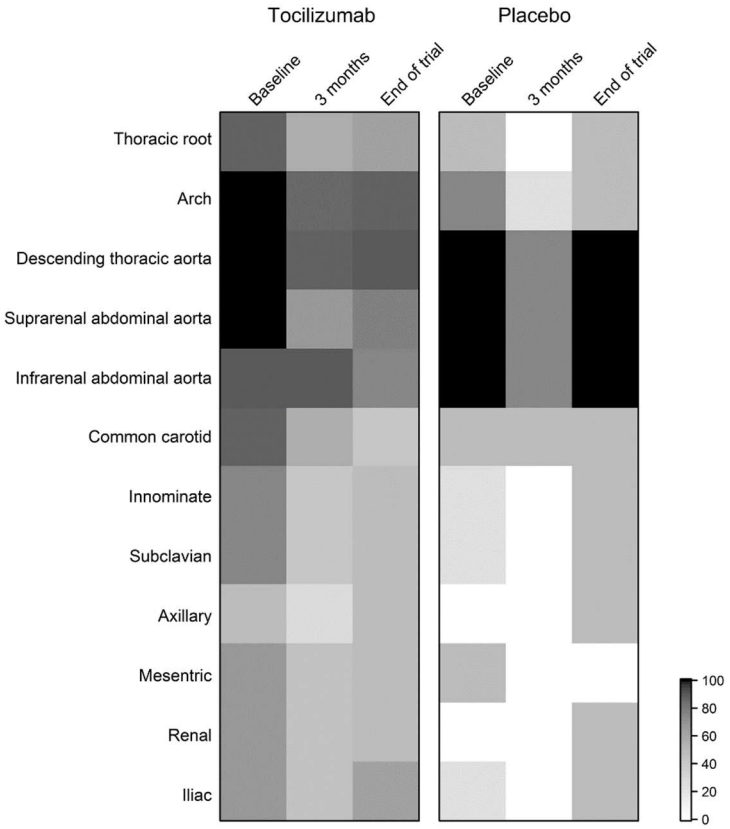

Reichenbach S, et al. Rheumatology doi:10.1093

Giant cell arteritis: pathogenic mechanisms and new potential therapeutic targets. Koster M, Warrington K.

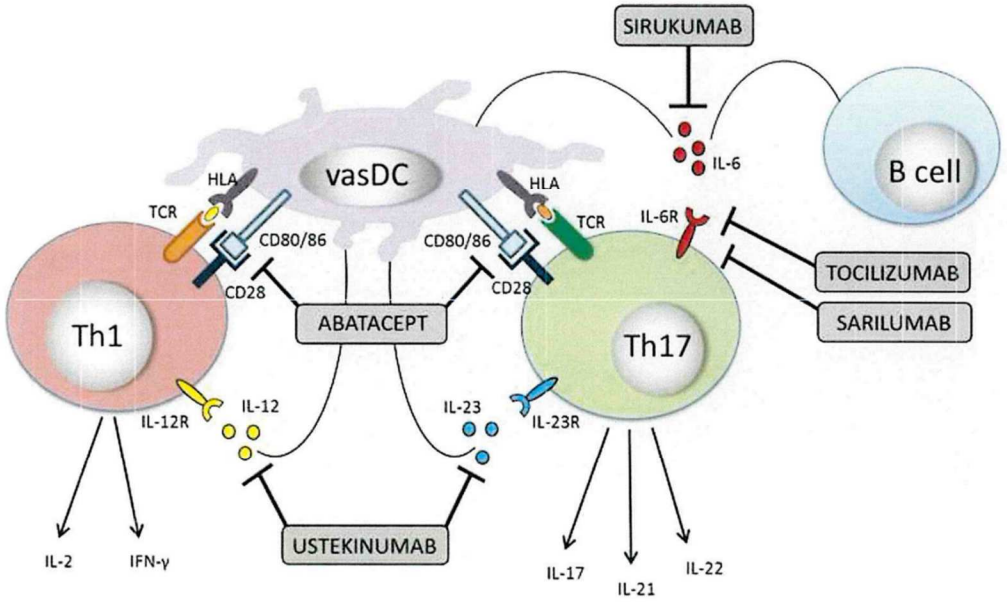

Ustekinumab for the treatment of refractory giant cell arteritis.

Conway R, O'Neill L, O'Flynn E, Gallagher P, McCarthy GM, Murphy CC, Veale DJ, Fearon U, Molloy ES.

Characteristics and prior treatment of 14 patients with Giant Cell Arteritis (GCA), treated with ustekinumab

Age, years, mean (SD)	69.6 (8.6)
Female, n (%)	11/14 (79)
Met 1990 ACR criteria for GCA, n (%)	14/14 (100)
Biopsy positive, n (%)	9/14 (64)
Temporal artery ultrasound positive, n (%)	3/10 (30)
CT Angiogram positive, n (%)	7/10 (70)
Cranial ischaemic complications, n (%)	3 (21%)
Vasculitis damage index, median (IQR)	2 (0, 2)
Charlson comorbidity index, median (IQR)	1 (1, 2)
Disease duration, months, median (IQR)	29.5 (12.8, 45.5)
Relapses, median (IQR)	2 (2, 4.3)
Clinical presentation at last relapse	
Cranial, n (%)	8 (57)
Polymyalgia rheumatica, n (%)	6 (43)
Constitutional, n (%)	6 (43)
Large vessel vasculitis, n (%)	5 (36)
Prior treatment	
Glucocorticoids, n (%)	14 (100)
Glucocorticoid adverse events, n (%)	12 (86)
Other immunosuppressants, n (%)	12 (86)
Other immunosuppressants failed, median (range)	1 (0, 3)
Methotrexate, n (%)	11 (83)
Duration of methotrexate, months, median (IQR)	10 (5, 36)
Dose of methotrexate, mg/week, median (IQR)	20 (15, 21)
Azathioprine	2 (14)
Leflunomide	1 (7)
Adalimumab	1 (7)

Ann Rheum Dis. 2016 Aug;75(8):1578-9.

Ustekinumab for the treatment of refractory giant cell arteritis.

Conway R, O'Neill L, O'Flynn E, Gallagher P, McCarthy GM, Murphy CC, Veale DJ, Fearon U, Molloy ES.

Table 2 Outcome measures pre-ustekinumab and at last follow-up (median follow-up of 13.5 months (range 7–26) after initiation of ustekinumab)

Outcome	Pre-ustekinumab	Last follow-up	p Value
Prednisolone dose, mg, median (IQR)	20 (15, 25)	5 (2.9, 8.1)	0.001
ESR, mm/h, median (IQR)	14 (5.8, 29.3)	15 (9.8, 28.5)	0.572
CRP, mg/L, median (IQR)	12.2 (3.4, 21)	4.8 (2.8, 15)	0.177
Stopped glucocorticoids, n (%)	–	4 (29)	–
Stopped other immunosuppressants, n (%)	–	11 (92)	–

CRP, C reactive protein, normal range 0–5 mg/L; ESR, erythrocyte sedimentation rate, normal range 0–30 mm/h.

Ann Rheum Dis. 2016 Aug;75(8):1578-9.

Interleukin-1 blockade in refractory giant cell arteritis.

Ly KH, Stirnemann J, Liozon E, Michel M, Fain O, Fauchais AL.

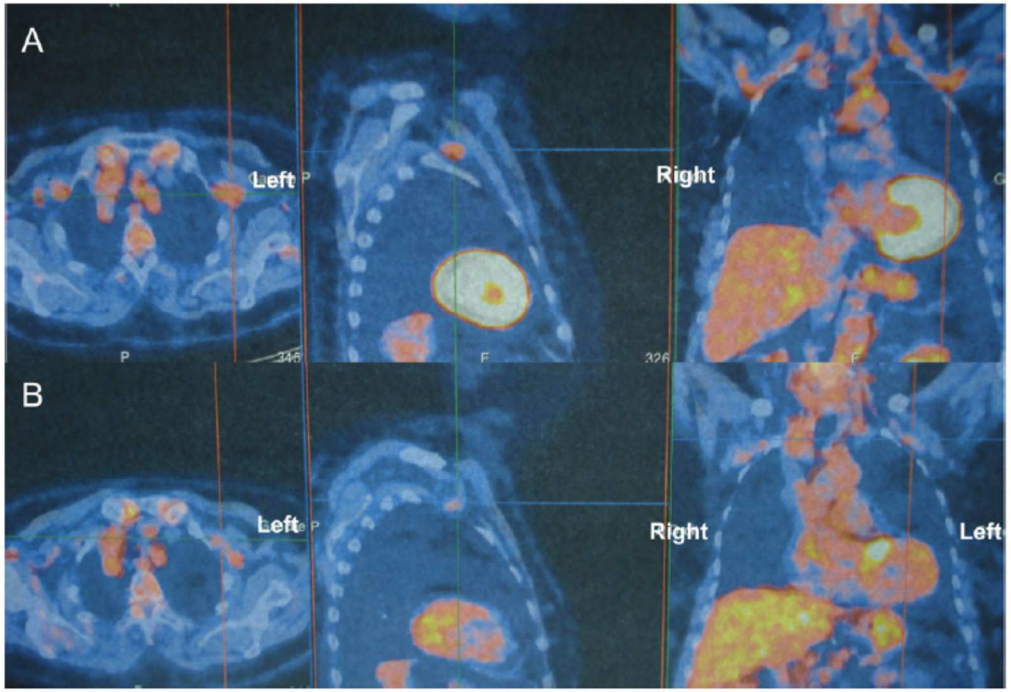

Fig. 1. PET/CT scans before (A) and 11 months after (B) anakinra treatment in the second patient, with markedly diminished of glucose uptake.

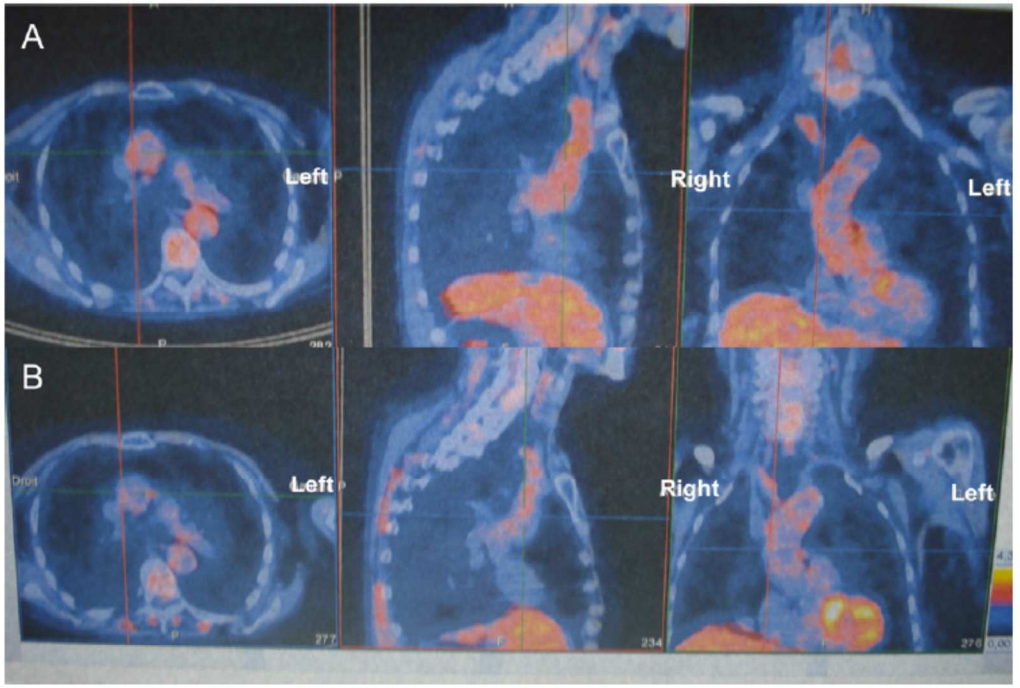

Fig. 2. PET/CT scans before (A: August 2011) and after anakinra treatment (B: January 2012) in the third patient showing less aortic inflammation.

Joint Bone Spine. 2014; 81: 76-8.

JAK–STAT Signaling as a Target for Inflammatory and Autoimmune Diseases: Current and Future Prospects

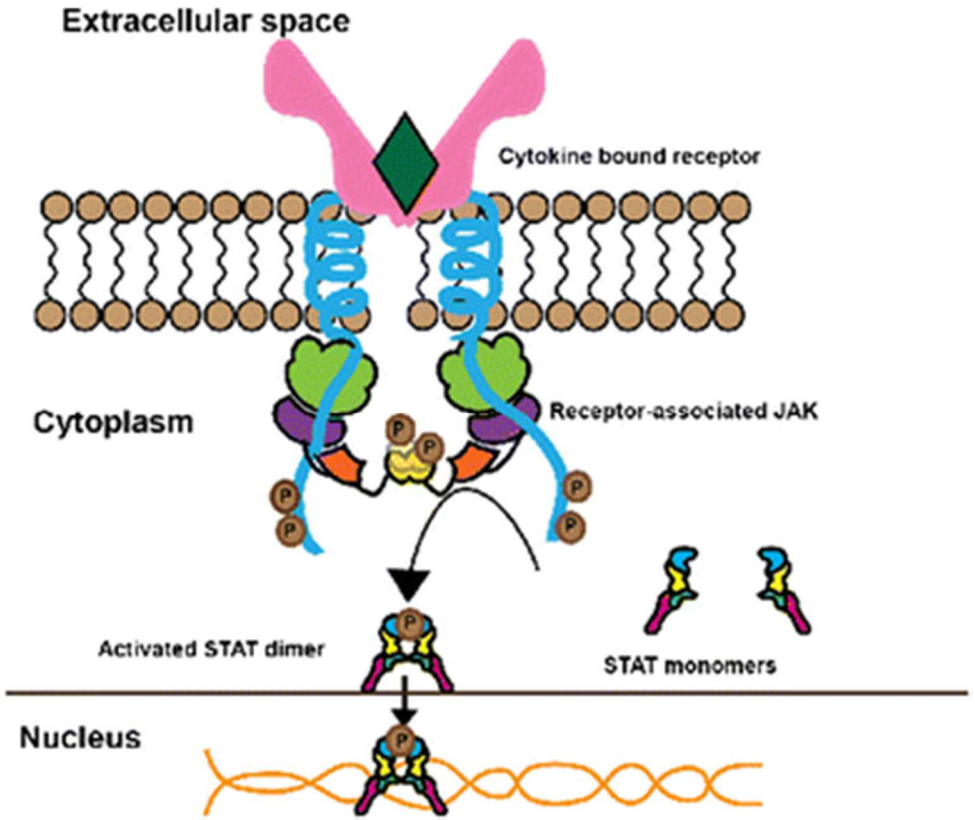

Banerjee S, Biehl A, Gadina M, et al. Drugs. 2017; 77(5): 521-546.

JAK–STAT Signaling as a Target for Inflammatory and Autoimmune Diseases: Current and Future Prospects

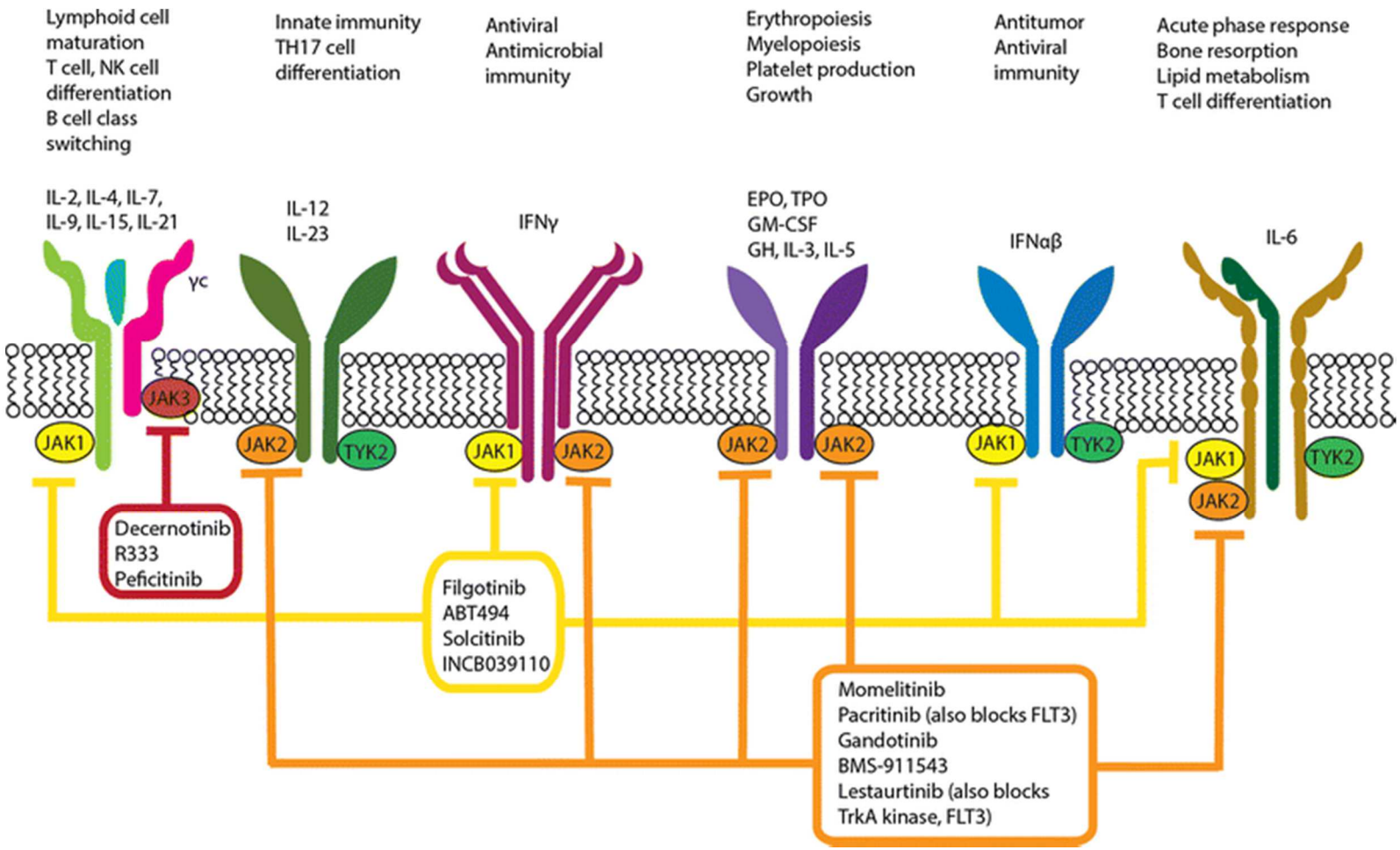

Banerjee S, Biehl A, Gadina M, et al. Drugs. 2017; 77(5): 521-546.

Inhibition of JAK-STAT Signaling Suppresses Pathogenic Immune Responses in Medium and Large Vessel Vasculitis.

Zhang H, Watanabe R, Berry GJ, Tian L, Goronzy JJ, Weyand C.

Background -Giant cell arteritis (GCA), a chronic autoimmune disease of the aorta and its large branches, is complicated by aneurysm formation, dissection, and arterial occlusions. Arterial wall dendritic cells (DC) attract CD4+ T-cells and macrophages (Mo), to form prototypic granulomatous infiltrates. Vasculitic lesions contain a diverse array of effector T-cells that persist despite corticosteroid therapy and sustain chronic, smoldering vasculitis. Transmural inflammation induces microvascular neoangiogenesis and results in lumen-occlusive intimal hyperplasia. We have examined whether persistent vessel wall inflammation is maintained by lesional T-cells, including the newly identified tissue-resident memory T cells (TRM) and whether such T-cells are sensitive to the cytokine signaling inhibitor tofacitinib, a JAK inhibitor (Jakinib) targeting the Janus kinase (JAK) 3 and JAK1. **Methods** -Vascular inflammation was induced in human arteries engrafted into immunodeficient mice that were reconstituted with T-cells and monocytes from GCA patients. Mice carrying inflamed human arteries were treated with tofacitinib or vehicle. Vasculitic arteries were examined for gene expression (RT-PCR), protein expression (immunohistochemistry) and infiltrating cell populations (flow cytometry). **Results** -Tofacitinib effectively suppressed innate and adaptive immunity in the vessel wall. Lesional T-cells responded to tofacitinib with reduced proliferation rates (<10%) and minimal production of the effector molecules IFN-γ, IL-17 and IL-21. Tofacitinib disrupted adventitial microvascular angiogenesis, reduced outgrowth of hyperplastic intima and minimized CD4+CD103+ tissue-resident memory T-cells. **Conclusions** -Cytokine signaling dependent on JAK3 and JAK1 is critically important in chronic inflammation of medium and large arteries. The Jakinib tofacitinib effectively suppresses tissue-resident memory T-cells and inhibits core vasculitogenic effector pathways.

Circulation. 2017 Dec 18.

Giant Cell Arteritis: From Pathogenesis to Therapeutic Management

Ryu Watanabe, Jörg J. Goronzy, Gerald Berry, Y. Joyce Liao, Cornelia M. Weyand

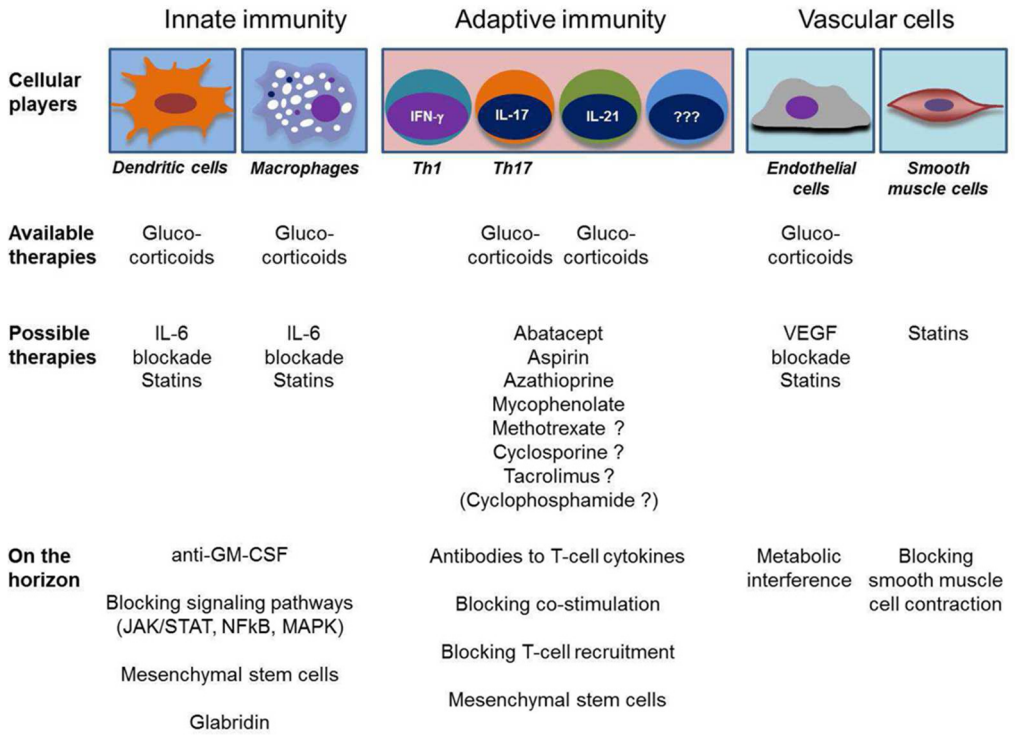

Curr Treat Options in Rheum 2016; 2: 126–137.

“Nature had millions of years to develop such a versatile immunosuppressant as glucocorticoids. It will take some time to design a cocktail of man-made immunomodulators that have equal efficacy”

Cornelia Weyand

Giant Cell Arteritis : from pathogenesis to therapeutic management. Curr Treatm Opt Rheumatol 2016; 2: 126-37